이학박사학위논문

암 억제인자 **BRCA2** 에 의한 텔로미어 유지기작 연구

Study on the functions of BRCA2 in the telomere maintenance

2013년 2월

서울대학교 대학원
생명과학부

민재원

암 억제인자 BRCA2에 의한 텔로미어 유지기작 연구

-Study on the functions of BRCA2 in the telomere maintenance-

指導敎授 李 賢 淑

이 論文을 理學博士學位論文으로 提出함

2012年 11月

서울大學校

生命科學部

閔 載 元

閔載元의 理學博士學位論文으로 認准함

2012年 12月

委 員 長 이 공 호

副委員長 이 현 숙

委 員 정 인 천

委 員 정 종 길

委 員 조 윤 제

Study on the functions of BRCA2 in the telomere maintenance

by

Jaewon Min

Advisor : Professor Hyunsook Lee, Ph.D

A Thesis submitted in Partial Fulfillment
of the Requirements for
the Degree of Doctor of Philosophy

February, 2013

School of Biological Sciences

Seoul National University

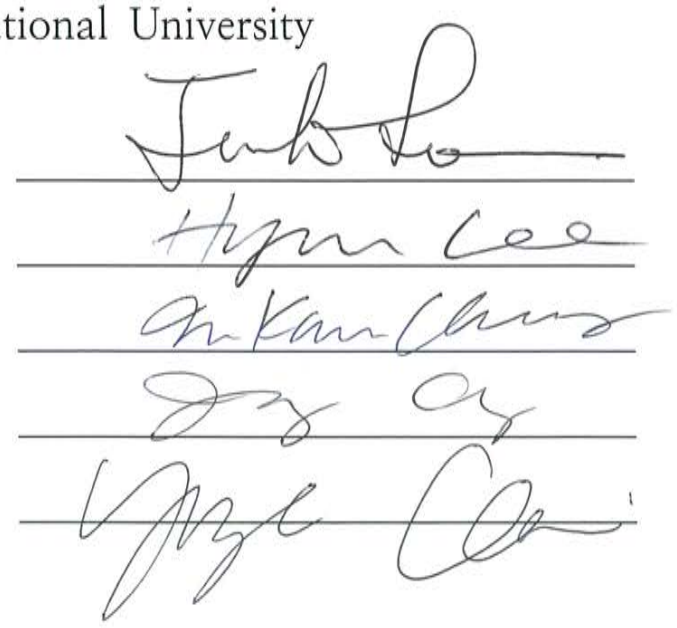

ABSTRACTS

Study on the functions of BRCA2 in the telomere maintenance

Jaewon Min

School of biological science

Seoul National University

Germ-line mutations in *BRCA2* predispose humans to cancers in the breast, ovary, and pancreas. Since BRCA2 is a key mediator of homologous recombination (HR) regulating Rad51 recombinase, absence of BRCA2 results in the accumulation of spontaneous gross chromosomal rearrangements (GCR) such as translocations, deletions, inversions and amplifications, which promotes tumorigenesis. It has been thought that such genetic alterations are originated from BRCA2's functional defect in HR or Stalled replication fork protection.

Here, I suggest that BRCA2 is involved in the maintenance of telomere homeostasis. Furthermore, absence of BRCA2 in a telomerase-deficient organism induces Alternative lengthening of telomeres (ALT), which is the alternative mechanism to protect itself from critical telomere shortening independent from telomerase.

Dysfunctional telomeres occurred in BRCA2-deficient cells in the form of end-to-end fusions, signal free ends, and anaphase bridges. I observed telomere length rapid deletion (TRD) in BRCA2-deficient MEFs, which is responsible for end chromosomal fusions. In search for the mechanistic basis of telomere shortening in the absence of BRCA2, I found that the replication fork stalling in telomeres was more profound compared to the non-telomeric region in BRCA2-knockout MEFs. For BRCA2 to function at telomeres, ATR was required. Specifically, BRCA2 has a role in facilitating G-rich lagging strand synthesis at telomeres, by blocking stalled replication fork degradation. Moreover, the fidelity of telomeric DNA replication is impaired in BRCA2-lacking condition. Theses data demonstrate that BRCA2 is required for the prevention of replication fork collapse at the telomeres. Accordingly, I conclude that the tumor suppressive function of BRCA2 involves the role at the telomere replication homeostasis.

If BRCA2 absence results in telomere shortening, how can BRCA2-deficient cells transform? By using the *C. elegans* model organism, I show that *C. elegans brc-2,* an orthologue of BRCA2 suppresses the induction of ALT. *brc-2* RNAi in *trt-1(ok410)* overcomes the short life-span in trt-1 mutant worms. *trt-1; brc-2* (RNAi) was capable of maintaining telomere length and displayed increased c-circles, indicating that ALT was induced. These results

indicate that absence of BRCA2 causes shortening of telomeres. Then at a critical point, absence of BRCA2 induces ALT, strongly suggesting that BRCA2 is the long-sought suppressor of ALT.

My study has shown how telomere shortening can induce genetic instability. Furthermore, these findings that BRCA2 is a suppressor of ALT implies how dysfunctional BRCA2 leads to cancer.

Keywords: BRCA2, telomere, genetic instability, tumorigenesis, ALT

Student number: 2009-30082

CONTENTS

LIST OF FIGURES

I. Introduction

I-1. The breast cancer susceptibility gene, BRCA2 is critical in Genetic integrity

I-1-1. The breast cancer susceptibility gene, BRCA2

BRCA2 is a tumor suppressor, responsible for the inherited susceptibility to early-onset breast and ovarian cancers (Tavtigian et al., 1996; Wooster et al., 1995). It is reported that the populations of *BRCA2* founder mutations possess higher tumor incidence when compared to non-carriers. In addition, germ-line heterozygosity of *BRCA2* mutations is sufficient for cancer predisposition. At least 800 mutations in the BRCA2 gene are found in breast cancer, ovarian cancer, prostate cancer, testicular cancer, fallopian tube cancer, male breast cancer, pancreatic cancer, and melanoma patients. Most mutations are generated from nonsense mutation, frame-shift mutation due to small insertion/deletion events, mutation within splice sites and germ-line mutations from genome rearrangement (Fackenthal and Olopade, 2007). The *Ashkenazi Jewish population* (6174delT) is a well-known founder mutation, which occupy 1.5% of their total population and possess high tumor incidence (-29% of ovarian cancer, -3% of breast cancer). The *Iceland population* (999del5) is

also a well-known founder mutation, which occupies 0.6% of their total population and possess high tumor incidence (-8% of ovarian cancer, -40% of male breast cancer).

It is known that the loss of checkpoint before the inactivation of the second *BRCA2* allele is a requisite for BRCA2-related tumorigenesis; however, the detailed processes underlying the carcinogenesis in the *BRCA2* mutation status is not yet fully understood. It is expected that the *BRCA2* mutation is a cancer susceptibility single-gene disorder, which provides a model for investigating the mechanisms of tumorigenesis (Venkitaraman, 2009). To resolve the process and consequence of BRCA2-related tumorigenesis, various types of Brca2 knock-out mouse models, targeting different regions, were generated (Evers and Jonkers, 2006). $Brca2^{Tr/Tr}$ mice, which carry a biallelic truncation in Brca2, display severe embryonic lethality and thymic lymphomas between 12 to 14 weeks (Friedman et al., 1998). The mouse embryonic fibroblasts from this mouse model exhibit aneuploidy as well as structural aberration in chromosomes (Venkitaraman, 2002). And *BRCA2* mutant cells are sensitive to ionizing radiation, and it has been revealed that *BRCA2* is also involved in homologous recombination (Patel et al., 1998). BRCA2-deficient cells spontaneously accumulate gross chromosomal rearrangements (GCR) such as translocations, deletions, inversions and amplifications (Yu et al., 2000). In the BRCA2-deficient condition, GCR formation is encouraged and genetic

instability induced from this condition would promote tumorigenesis (Venkitaraman, 2009). Recent reports show that BRCA2 regulates the spindle assembly checkpoint through reinforcement of BubR1 acetylation (Choi et al., 2012). Based on these data, we can easily assume that BRCA2 is involved in the maintenance of genetic integrity.

In contrast with a mono-allelic *BRCA2* mutation, which induces hereditary tumor, a biallelic *BRCA2* mutation is associated with Fanconi anemia (Venkitaraman, 2004). Fanconi anemia is a rare genetic cancer-susceptibility syndrome that is characterized by bone marrow failure, abnormal skin pigmentation, and various developmental abnormalities (Kennedy and D'Andrea, 2005). Until now, 15 Fanconi anemia complementation group [A, B, C, D1 (***BRCA2***), D2, E, F, G, I, J (BRIP1), K, L, M, N (PALB2), O (RAD51B), P (SLX4)] have been cloned. Cells derived from FA patients exhibit chromosomal instability and hypersensitivity to DNA cross-linking agents, such as mitomycin C (MMC), cisplatin (CDDP), and diepoxybutane (DEB) which indicate that the FA pathway is involved in inter-crosslink repair (ICR) (Venkitaraman, 2004). Since ICR mechanisms are required for the coordination of nucleotide excision repair (NER), homologous recombination (HR), and translesion repair (TLR), *BRCA2*-mutation indeed exhibits ICR defects.

I-1-2. The role of BRCA2 in homologous recombination and stalled replication fork protection

From the smut fungus *Ustilago maydis* to humans, the *BRCA2* orthologue has been found. It has been revealed that BRCA2 protein possesses the evolutionary conserved BRC repeat, which interacts with recombinase Rad51 which is required for homologous recombination (Pellegrini and Venkitaraman, 2004; Venkitaraman, 2002; West, 2003) Homologous recombination is an error-free DSB repair pathway which uses the sister chromatid as a template, during S or G2 phases of the cell cycle (Venkitaraman, 2009) (**FIGURE 1**). *U. maydis BRCA2* and *C. elegans BRCA2* have one BRC motif, *Drosophila melanogaster BRCA2* has three BRC motifs, *Arabidopsis thaliana BRCA2* has four BRC motifs, Chicken *BRCA2* has six BRC motifs, and mouse and human *BRCA2* have eight BRC motifs. In X-ray crystallography, BRC repeats in the human exon 11, bind to the ATPase-core domain of Rad51, and mimic the binding motif of Rad51, inhibiting the oligomerization of Rad51 in heptameric structure (Pellegrini et al., 2002). And in EMSA experiments, BRC repeats bind to monomeric Rad51 in at a high molar ratio, but to oligomerized Rad51 filaments for strand invasion in at a low molar ratio (Galkin et al., 2005; Shivji et al., 2006). These results suggest that BRC repeats of BRCA2 regulate Rad51 both positively

(loading Rad51 onto ssDNA) and negatively (Rad51-filament dissociation after strand invasion) in homologous recombination.

In the TR2 region in exon27, another Rad51 binding motif that serves as an interface for Rad51 filaments stabilization has been identified (Esashi et al., 2005; Esashi et al., 2007). However, the TR2 region is dispensable for homologous recombination. The function of the TR2 motif was recently identified as stalled replication fork protection from MRE11-dependent resection. The BRCA2-Rad51 filaments complex protects the stalled replication fork from MRE11-dependent resection **(FIGURE 2),** which is distinguished from the homologous recombination function, as RAD54 **(a motor protein involved in homologous recombination; holliday junction branch migration, Rad51-filament dissociation)** is not involved in stalled replication fork protection.

Figure 1.

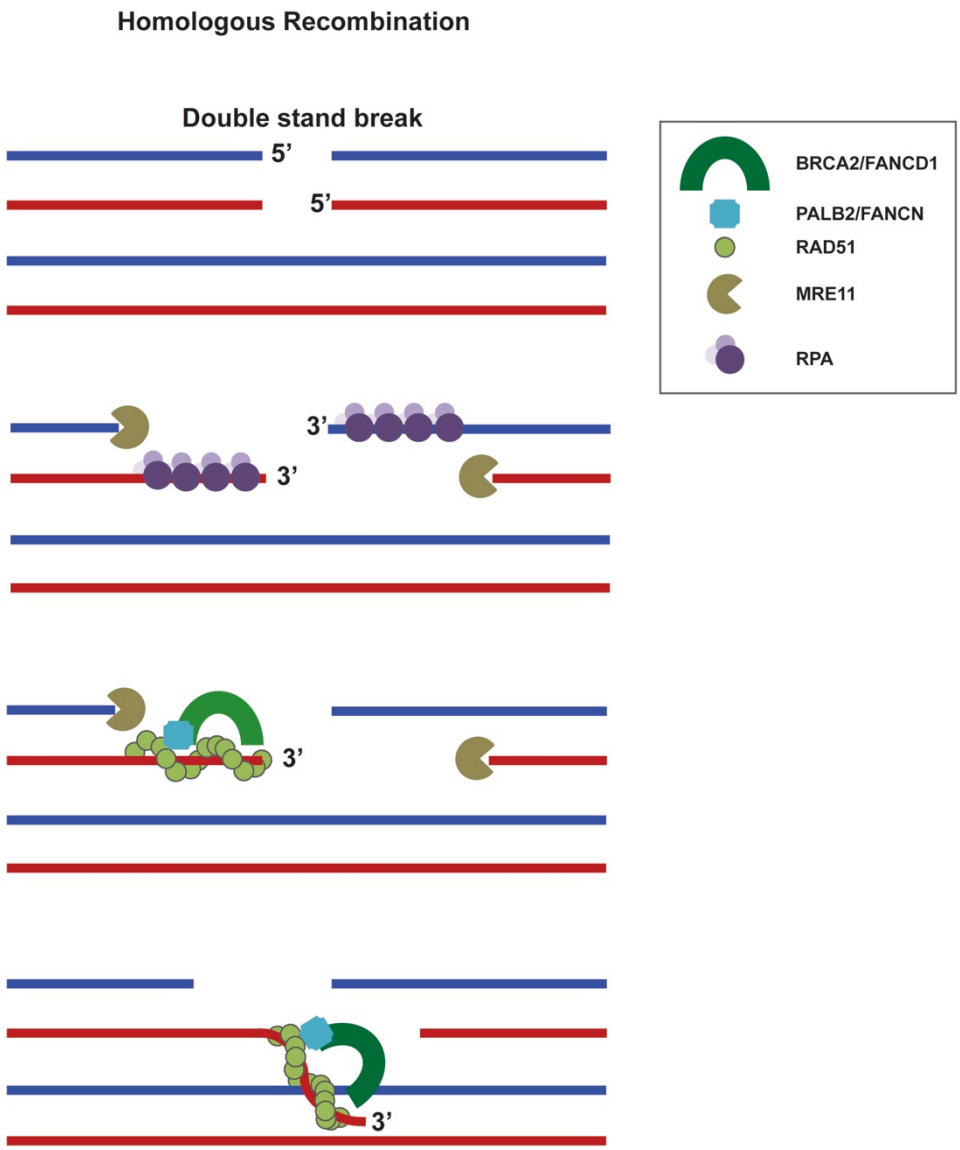

Figure 1 The roles of BRCA2 in Homologous recombination

Figure 1. The roles of BRCA2 in Homologous recombination

Model for the roles of BRCA2 in homologous recombination, an error-free DNA Double strand breaks (DSBs) repair. DNA DSBs activates the ATM pathway and recruits the MRN complex, which resects DSB ends to generate 3' single stranded DNA (ssDNA) overhangs. Exposed 3` ssDNA overhangs are coated by RPA proteins, which are stimulated by ATR pathways. BRCA2 promotes the RAD51 filament formation on RPA-coated 3' ssDNA overhangs to perform homologous sequence search and DNA strand invasion (Liu et al., 2010). Strand invasion by 3` ssDNA overhangs into a homologous sequence is mediated by the BRCA2-PALB2 / RAD51-filaments complex.

Figure 2.

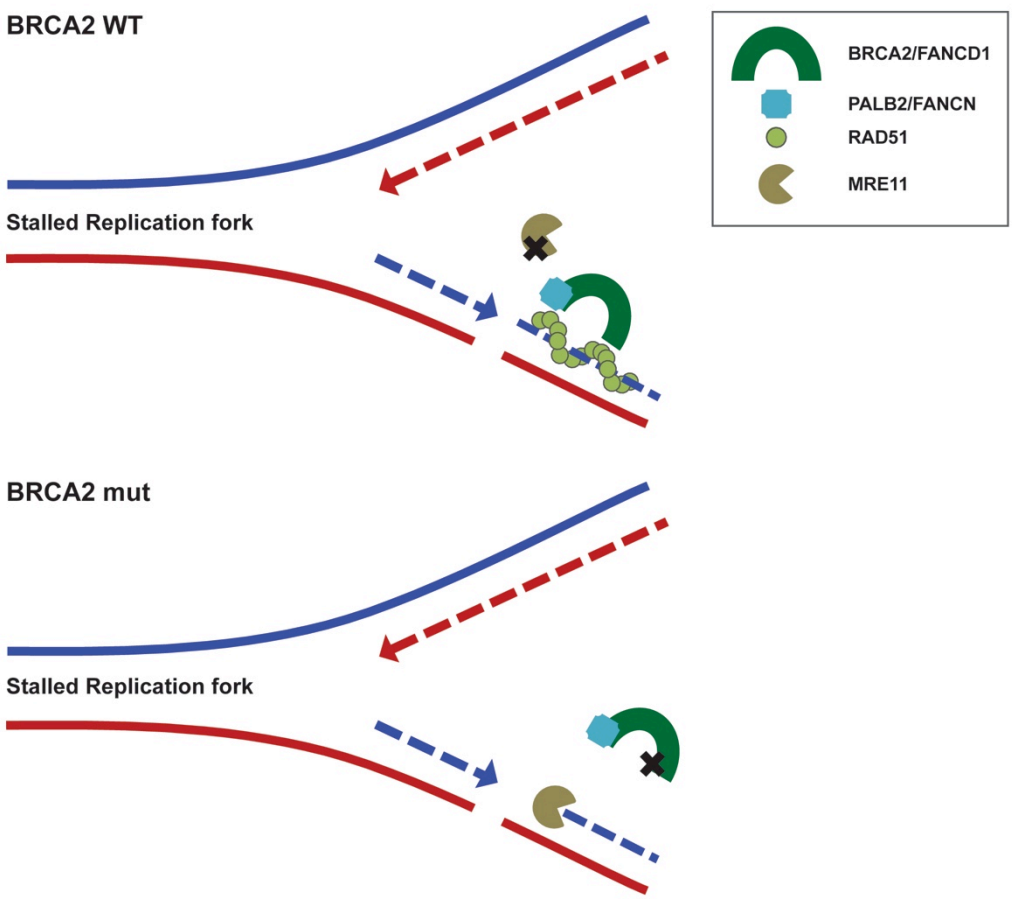

Figure 2 The roles of BRCA2 in stalled DNA replication fork protection

Figure 2. The roles of BRCA2 in Stalled DNA replication fork protection

Model for the roles of BRCA2 in blocking stalled replication fork degradation by MRE11 (Schlacher et al., 2011), which are homologous recombination-independent roles. In wild-type cells, which express intact BRCA2, BRCA2 stabilizes RAD51 filaments on stalled replication forks, until the replication stall is removed. In BRCA2-mutated cells, nascent strands of the stalled fork are unprotected and degraded by MRE11 exonuclease.

I-2. Telomere maintenance mechanisms

I-2-1. Telomere, the TTAGGG(C) repetitive sequence at the end of chromosomes

A Telomere is the TTAGGG repetitive sequence at the end of chromosome and operates to prevent chromosome ends from being recognized as DNA double strand breaks (DSB) **(FIGURE 3).** An Unprotected telomere activates the DNA damage response pathway and promotes efficient NHEJ of dysfunctional telomeres, which leads to end-to-end fusion. Telomeres are shortened with cell division, which is referred to as the end replication problem. Most normal cells show progressive telomere shortening with ongoing cell division until telomeres reach a critical short length that induces checkpoint activation and senescence. Telomerase, an RNA-containing (-AAUCCC-) enzyme, synthesizes telomere sequence onto the ends of G-overhang sequences. Telomerase is silent in most human tissue and is only expressed in germ-line cells and a subset of proliferating somatic adult progenitor cells (Wright et al., 1996).

Figure 3.

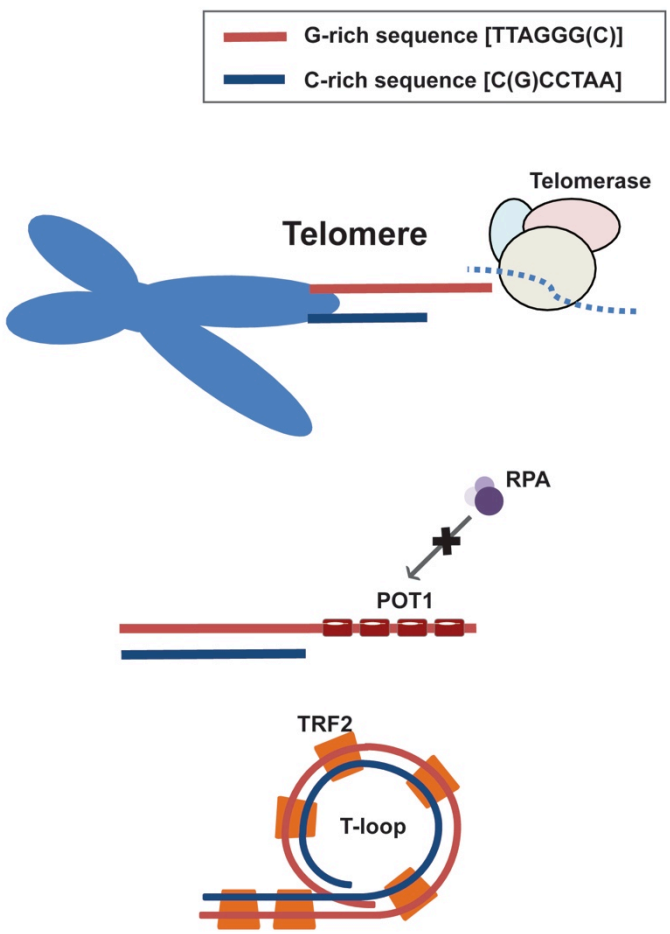

Figure 3 Telomere, TTAGGG(C) repetitive sequence at the end of chromosomes

Figure 3. Telomere, the TTAGGG(C) repetitive sequence at the end of chromosomes

A Telomere is a repeating DNA sequence at the end of the chromosomes. Telomeres function by preventing chromosomes from losing DNA sequences at the ends. Telomerase is a ribonucleoprotein enzyme complex (composed of an RNA template (TERC), catalytic subunit (TERT), dyskerin, and NOP10). Telomerase maintain telomere length by adding (TTAGGG) sequences onto the telomeric ends of the chromosomes, thus compensating for the end replication problem. Due to telomeres being located at the end of chromosomes, shelterin proteins are localized at the telomeres to protect DNA ends from being recognized as DNA damage sites. POT1 protects telomeres from the ATR-dependent DNA damage response by preventing the binding of RPA to the 3'-overhang (Wu et al., 2006). TRF2 protects telomeres from an ATM-dependent DNA damage response by mediating T-loop formation (Griffith et al., 1999).

I-2-2. Molecular mechanism of Telomere replication fidelity

Replication of telomere is unidirectional as replication forks originate from subtelomeres, moving towards chromosome ends (Gilson and Geli, 2007; Sfeir et al., 2009) **(FIGURE 4).** Due to unidirectional replication fork progression, telomeres possess the G-rich strand as the parental lagging strand, and the C-rich strand as the parental leading strand, and therefore stalled replication forks cannot be rescued by converging with another replication fork. Furthermore, telomeres face difficulty in the DNA replication process because repetitive arrays of G-rich DNA sequences in telomeres can make higher order structures such as the G-quadruplex. It has been suggested that a G-rich parental lagging strand would adopt higher order structures, such as the G-quadruplex, when it becomes single-stranded in the region between okazaki fragments. Recently, it has been reported that telomeres are prone to cause trouble in replication fork progression, which result in telomeres resembling fragile sites (Sfeir et al., 2009). Hence the prevailing mechanisms involved in the repair and restart of a stalled replication fork are essential for telomeric DNA replication. Incomplete telomere replication resulting from replication fork aberrations would lead to severe telomere length shortening and end capping problem (Gilson and Geli, 2007). Critically short or uncapped telomeres induced by incomplete telomere replication activate the DNA damage response pathway and promotes efficient NHEJ of dysfunctional telomeres, followed by end-to-

end fusion. Chromosomal end fusions precede breakage-fusion-bridge (BFB) cycles, which generate various types of structural abnormalities that would result in gene deletion and gene amplification. Such alterations are regarded as genetic instability, a hallmark of cancer.

Hence, it has been considered that the maintenance of telomere replication fidelity is crucial for genetic integrity. One example, the Werner syndrome (WS), is a disorder where Werner-deficient cells exhibit premature aging and high-incidence cancer phenotypes. This disorder is caused by mutations in the gene encoding the RecQ helicases WRN, which are essential for preventing telomere loss during telomere replication (Crabbe et al., 2007). WS cells display aberrant telomere phenotypes such as end-to-end fusions, signal-free ends and anaphase bridges, which results in genetic instability.

Figure 4.

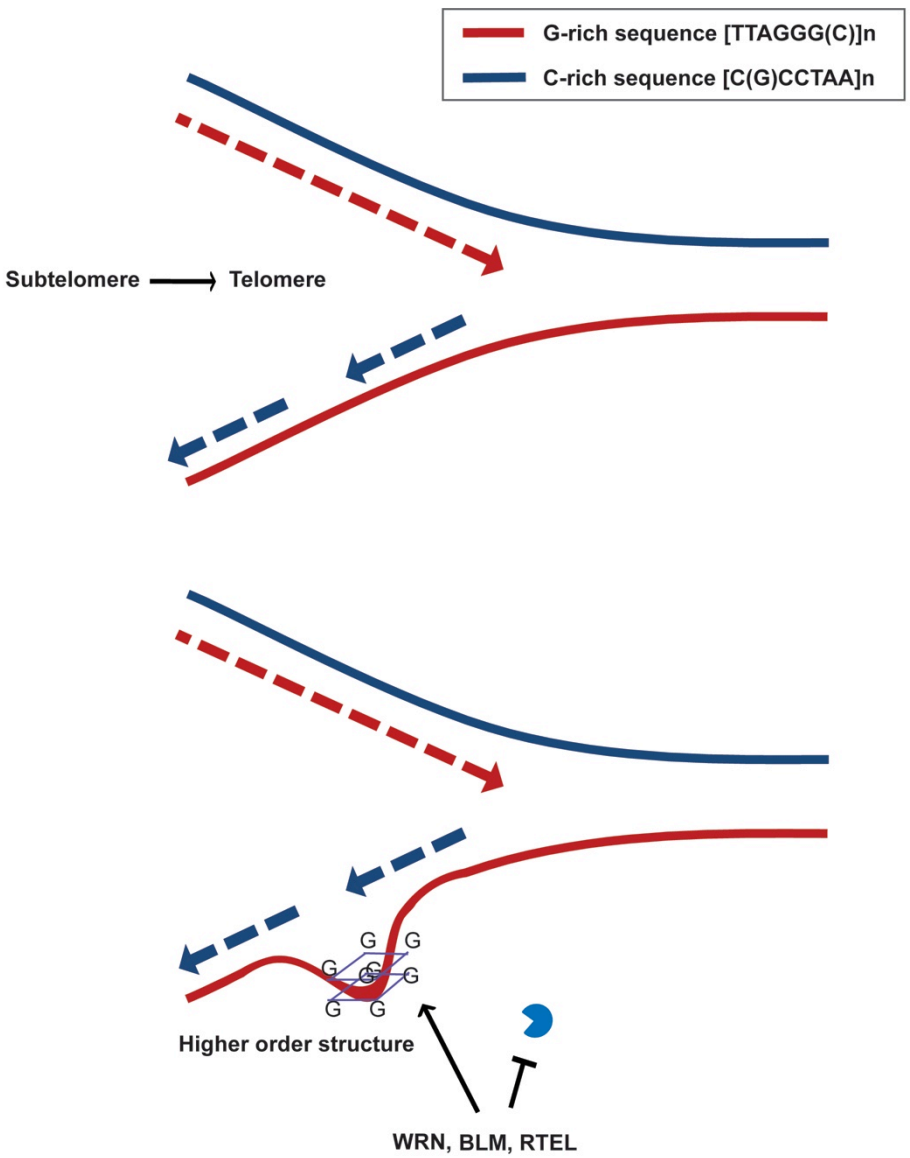

Figure 4 The mechanism of telomere replication

Figure 4. The mechanism of telomere replication

Since telomeres lack a DNA replication origin, replication forks at the telomeres are originated from the subtelomeres (regions adjacent to the telomeres) and move unidirectionally towards chromosome ends (Gilson and Geli, 2007; Sfeir et al., 2009). Due to unidirectional replication fork progression, telomeres possess the G-rich strand as the parental lagging strand, and the C-rich strand as the parental leading strand, and therefore stalled replication forks at the telomeres cannot be rescued by converging with another replication fork.

Telomeres face difficulty in the process of DNA replication because repetitive arrays of G-rich DNA sequences in telomeres can make higher order structures such as the G-quadruplex. G-rich parental lagging strands adopt higher order structures, such as the G-quadruplex, when it becomes single-stranded in the region between Okazaki fragments. The helicase proteins, WRN, BLM, and RTEL, are localized at the telomeres to resolve the higher order structure.

I-2-3. Molecular mechanism of Telomere end capping

Telomeres protect their structure by forming large hairpin loop structures called telomere loops, or T-loops. The sizes of T-loop can vary greatly (1 kb~25 kb, in humans), which might depend on telomere length (de Lange, 2004). It has been suggested that T-loop formation and maintenance mechanisms are mediated by TRF2 or HR machinery **(FIGURE 5)**. T-loop-sized telomeric circles, called T-circles, are generated in the presence of a dominant negative-TRF2 (TRF2ΔB), in the absence of the HR machinery factor, or in the presence of the long telomeres (over-lengthened by telomerase or ALT onset condition) (Wang et al., 2004). The T-circle generation mechanism, called telomere trimming or trimming, induces rapid telomere length shortening by T-loop junction resolution, which is thought to be the negative regulatory mechanism for telomere length (Pickett et al., 2011). Telomere trimmings in normal telomere length conditions are the result of telomere uncapping (absence of TRF2 or HR machinery), and induce very shortened telomeres. Critically shortened telomeres induced by trimming generate NHEJ among very short telomeres, followed by end-to-end fusions.

Figure 5.

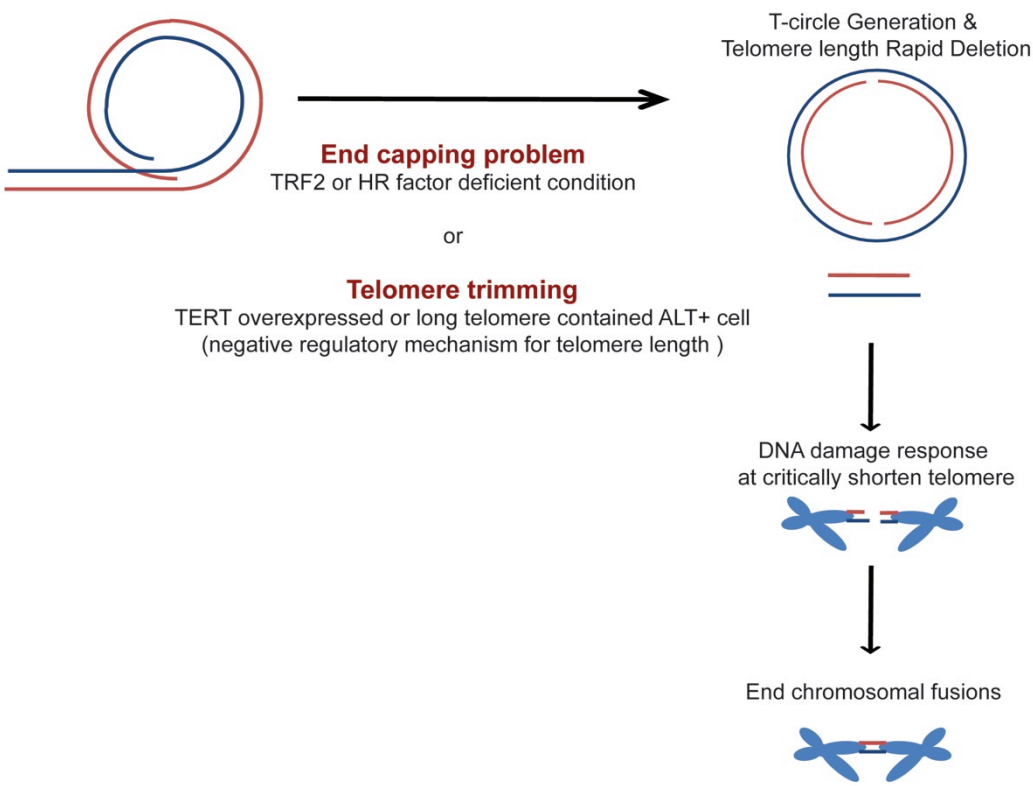

Figure 5 Telomere end-protection problem

Figure 5. Telomere end-protection problem

Telomeres protect their ends by remodeling linear DNA into T-loops. T-loops are dsDNA loop structures formed by the invasion of 3' overhangs into the duplex part of the telomere sequence. T-loops generate and maintain their structure by TRF2 or Homologous recombination (HR) machinery. T-circles are generated by a resolution of the T-loop junction, in response to the end capping problem (Defects in T-loop maintenance mechanism; TRF2- or HR factor deficient condition) or telomere trimming (negative regulatory mechanism for telomere length). T-circle generation induces T-loop-sized deletion, called the Telomere Rapid Deletion (TRD) (Wang et al., 2004). Critically shortened telomeres induced by TRD are recognized as DNA damage sites, and lead to end chromosomal fusions.

I-3. Telomere, genetic instability, and tumorigenesis

I-3-1. Telomere length shortening and tumorigenesis

The correlation between telomere length shortening and tumorigenesis has been modeled by dysfunctional telomere analysis in breast and colon cancer (Artandi and DePinho, 2010) **(FIGURE 6)**. Extended proliferation in the early stages of tumorigenesis comes with telomere shortening due to insufficient telomerase activity (Hackett and Greider, 2002). During human breast carcinogenesis, telomere length shortenings are prolonged. The occurrence of chromosomal instability and telomere erosions are increased as well (by BFB cycle). Telomerase onsets occur at the ductal carcinoma in situ stage where chromosomal instability and telomere erosions are reduced (Chin et al., 2004). Thus, it is expected that telomeres being shortened and becoming dysfunctional during the initiation stage of tumorigenesis can serve as a key mutation mechanism (Artandi and DePinho, 2010).

Here, I show that BRCA2 has critical roles in telomere maintenance. Absence of BRCA2 increases dysfunctional telomeres. Telomere erosion and shortening in BRCA2-deficient cells would contribute to increased DNA damage and genetic instability, leading to tumorigenesis. Accordingly, I can conclude that BRCA2 has critical roles in telomere maintenance, and illustrate

the contribution of telomere erosions to tumorigenesis in BRCA2-deficient cells.

Figure 6.

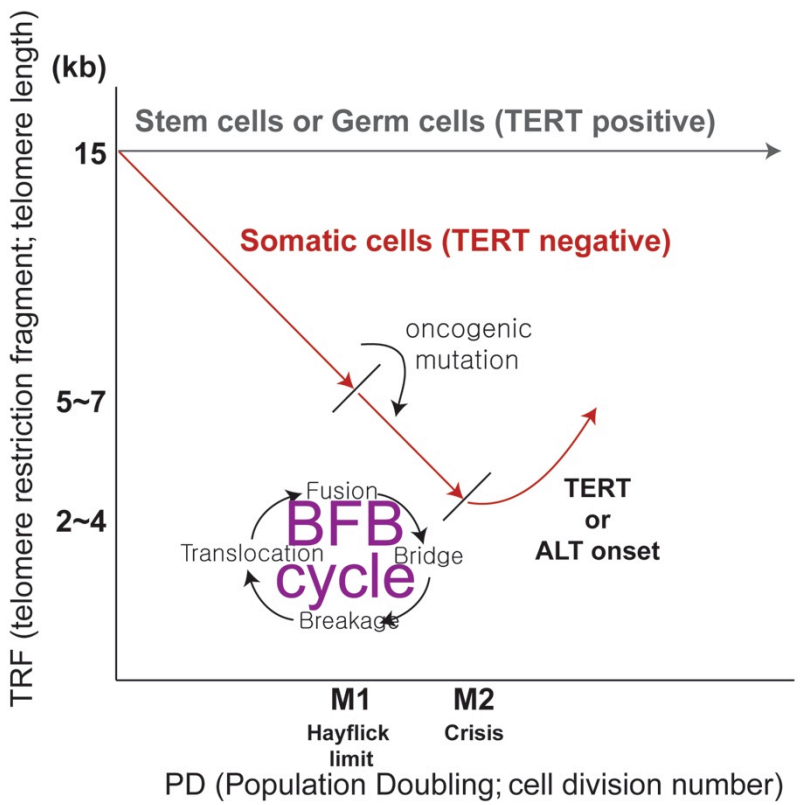

Figure 6 Telomere length shortening and genetic instability in tumorigenesis

Figure 6. Telomere length shortening and genetic instability in tumorigenesis

Model for the relationship between telomere length and neoplastic transformation (tumorigenesis)

In somatic cells, telomeres become shortened over successive cell divisions due to the end replication problem. In normal proliferating somatic cells, cell divisions accompany telomere length shortening progressively until it reaches a critical length (Hayflick limit, M1). If cell division persists despite the shortened telomere due to oncogenic mutations (cell cycle checkpoint, e.g. p53/pRB pathway), chromosome end fusions would be increased. Chromosome end fusions accelerate genetic instability by the break-fusion bridge cycle (BFB cycle) and cell divisions continue until they reach crisis (M2). Very rarely cells escape crisis by activating telomerase or acquiring alternative lengthening of telomeres (ALT) mechanisms, which reduces genetic instability. Then cells become cancer cells with unlimited division capacity.

I-3-2. Alternative lengthening of telomeres (ALT) in Cancer

Cell division accompanies telomere length shortening due to insufficient telomerase activity in most normal cells (end replication problem). Shortened telomeres induce a DNA damage response that leads to cell cycle arrest, known as senescence. Rarely, cells that acquired mutations such as checkpoint mutations avoid senescence (hayflick limit, **FIGURE 6** M1). Prolonged proliferation in the presence of shortened telomeres induces BFB cycles, leading to genetic instability. Infrequently, cells acquire a telomere maintenance mechanism by genetic changes for neoplastic transformation, which enhances the proliferation capacity of cancer cells (crisis, **FIGURE 6** M2). In cancer cells, telomeres can be maintained by telomerase activation (85 ~ 90 %) or alternative lengthening of telomeres (10 ~ 15 %) mechanisms. Thus, verifying the ALT mechanism is required for understanding how cancer cells counteract telomere shortening to sustain proliferative potential, which is the central issue regarding the properties of cancer.

Although the mechanisms for telomerase independent telomere lengthening, the alternative lengthening of telomeres, have not been identified clearly in metazoans, several ALT markers have been suggested **(FIGURE 7)**. T-circles **(FIGURE 7 -1)** are extra-chromosomal telomeric dsDNA structures, including double strand circles, linear double-stranded DNA, and highly branched

structures. PML bodies containing telomere DNA are referred to as APBs (ALT-associated PML bodies) **(FIGURE 7-2)**. T-SCEs (Telomere sister chromatid exchanges, **FIGURE 7-3**) are sister chromatid exchanges in the telomere region, and the elevation of T-SCE frequency in ALT cells is irrelevant with the elevation of SCE frequency in the genome. Although T-circles, APBs, and T-SCEs are frequently found in ALT cells and may be useful markers for ALT, they are not all equally specific for every ALT cell (**FIGURE 7**) (Cesare and Reddel, 2010).

C-circles are C-rich (CCCTAA) repetitive sequences containing circular ssDNA **(FIGURE 7-4)**. While unusual, most common ALT cell lines that lack some or most usual characteristic of ALT cell lines (T-circles, T-SCEs, APBs, heterogeneous telomere length) but maintain their telomere length with $TERT^{negative}$ nevertheless contain abundant C-circles, suggesting that C-circles are the most specific and quantifiable markers for ALT. C-overhangs are also abundantly found in ALT cells **(FIGURE 7-5)**. C-overhang generation is increased upon the depletion of HR factors (RAD51, RAD52) in ALT cells (Oganesian and Karlseder, 2011). Although C-circles and C-overhangs generation mechanisms and their features are not clearly elucidated, C-circles and C-overhangs could give conclusive clues for ALT mechanisms.

Based on ALT markers, several ALT mechanism models have been suggested **(FIGURE 8)**. Since elevated levels of T-SCEs in ALT cells indicate that a recombination-based mechanism is involved in ALT mechanisms, an Inter-telomere Homologous recombination-dependent DNA replication hypothesis (IHD) has been proposed **(FIGURE 8, upper)**. It has been suggested that homologous recombination mediates telomere DNA replication by using an adjacent long telomere as a template to elongate the short telomere. Although IHD is more suitable than other recombination based hypotheses, such as the unequal T-SCE model that does not result in a net increase in telomeric DNA, IHD still cannot explain the abundance of c-circles, c-overhangs in ALT cells. It has also been suggested that telomere DNA synthesis can be done by using a T-circle or C-circle as a template **(FIGURE 8, middle-bottom)**. T-circles and C-circles may be the template for telomere extension by the Rolling Circle Amplification (TMRCA or CMRCA) mechanisms. Strand invasion (using T-circle as a template) or annealing (using C-circle as a template) of G-rich overhangs to complementary strands in circles followed by DNA polymerization would promote extensive synthesis of G-rich strands at the chromosome ends. This model would be most fitting for explaining ALT mechanisms. However, there are several critical main questions for the RCA hypothesis as to which RCAs are preferred (TMRCA or CMRCA) and which overhang is used for elongation (C-overhang or G-overhang). **(FIGURE 25)**

Here, I show that *C. elegans brc-2,* an orthologue of BRCA2, suppresses the induction of ALT. *brc-2* RNAi in *trt-1(ok410)* induce the extended propagation. *trt-1; brc-2* (RNAi) were capable of maintaining telomere length and displayed increased c-circles, indicating that ALT was induced. Accordingly, I can conclude that BRCA2 is a suppressor of ALT, and illustrates the contribution of acquiring the ability for telomere length maintenance to tumorigenesis in BRCA2-deficient cells.

Figure 7.

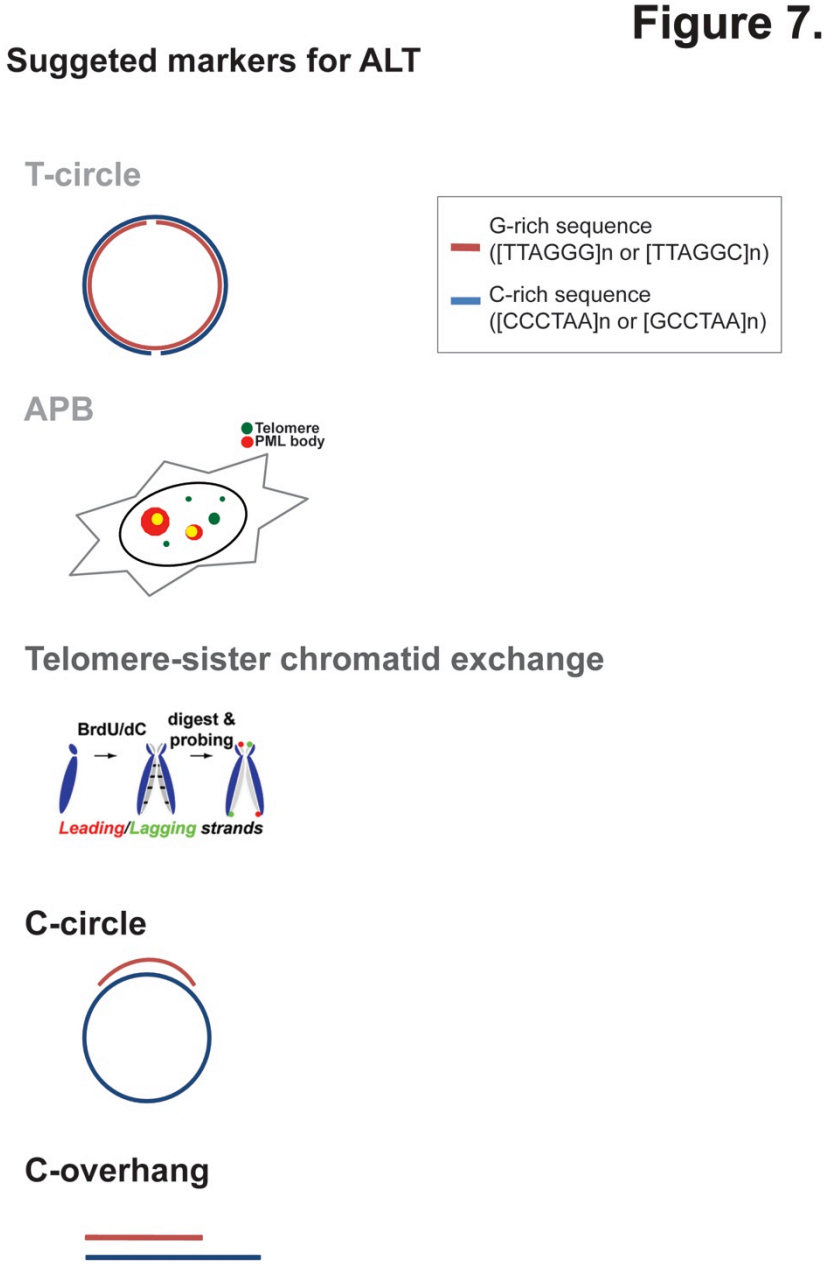

Figure 7 The suggested markers for Alternative Lengthening of Telomeres (ALT)

Figure 7. The suggested markers for Alternative Lengthening of Telomeres (ALT)

T-circles

Double stranded T-circles are generated from the resolution of telomere loop junctions. It has been initially suggested that T-circles are markers for ALT, due to the abundance of T-circles in ALT cells compared to non-ALT cells. However, it has been verified that telomere trimming, a negative regulatory mechanism for telomere length, generates T-circles. Therefore, abundant t-circle in ALT cells result from telomere trimming counteracting extensive ALT-mediated lengthening, and thus not relevant to the ALT mechanism (Cesare and Reddel, 2010).

APB

ALT-associated PML Bodies (APBs) represent colocalizations between PML proteins and telomeric DNA. Initially APBs have been referred to as ALT markers, however its features overlapped with those of telomere trimming mechanisms. Thus APBs are also considered as the result from telomere trimming counteracting extensive ALT-mediated lengthening, and not relevant to the ALT mechanism (Pickett and Reddel, 2012).

Telomere-sister chromatid exchange

Telomere sister chromatid exchange (T-SCE) occurs more frequently in ALT cells than in telomerase positive cell lines or normal cells. T-SCEs may result from recombination between intra-chromatids. However, T-SCEs do not result in a net gain of telomeric DNA as one sister chromatid is elongated at the expense of the other (Royle et al., 2009). T-SCEs are found in critically shortened telomeres containing normal or telomerase positive cells, and it also results from epigenetic alteration in normal telomeres. ALT cells contain nicked and gapped telomeric DNA that would lead to increased frequency of T-SCEs. Therefore, T-SCEs are ALT-phenotype-associated features, and not a exclusive marker for ALT cells.

C-circles

C-circles are C-rich (CCCTAA) repetitive sequences containing circular ssDNA. C-circles are found in the most ALT-characterized cells as well as in ALT cells that could not be characterized by other ALT markers. C-circles are exclusively found in ALT cells. Furthermore, ALT activity onset and C-circle generations occurred simultaneously. When ALT activity is inhibited, most C-circles disappeared within 24 hours (Cesare and Reddel, 2010).

C-overhangs

In normal cells, most telomeres contain G-overhangs (3' G-rich sequence). In humans, C-overhangs (5' C-rich sequence) are found abundantly in ALT cells. Although the C-overhangs generation mechanism and its features are not elucidated yet, in my opinion, C-overhangs could be a conclusive clue for ALT mechanisms with C-circles as well as a robust marker for the ALT phenotype.

Figure 8.

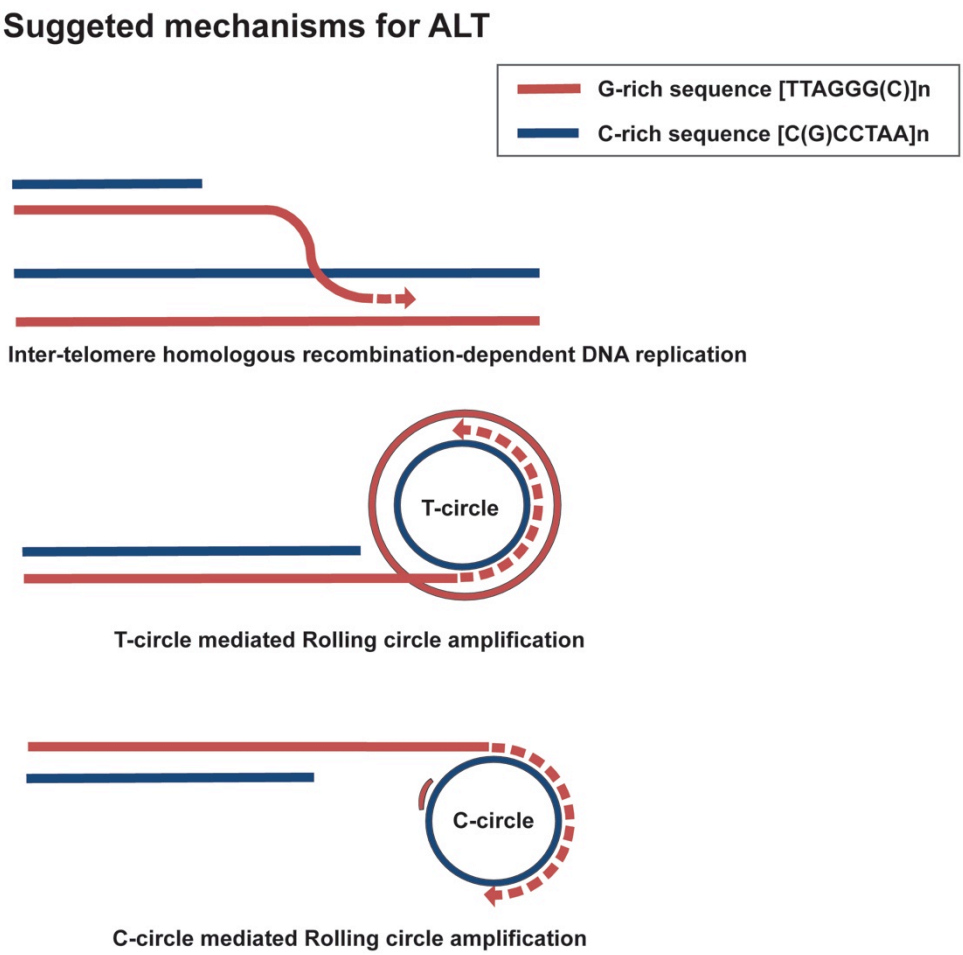

Figure 8 The suggested mechanisms for Alternative Lengthening of Telomeres

Figure 8. The suggested mechanisms for Alternative Lengthening of Telomeres

There are several hypotheses for ALT mechanisms, but none of them are certain due to insufficient evidence.

Inter-telomere homologous recombination-dependent DNA replication hypothesis

It has been suggested that alternative lengthening of telomeres can result from homologous recombination mediated telomere DNA synthesis using adjacent long telomeres as templates.

T-, C- circle mediated Rolling Circle Amplification hypothesis

It has been also suggested that telomere DNA synthesis by using a T-circle or C-circle as a template. T-circles and C-circles may be the templates for telomere extension by the Rolling Circle Amplification (RCA) mechanisms. Strand invasion (using T-circle as a template) or annealing (using C-circle as a template) of the G-rich overhang to complementary strands in circles followed by DNA polymerization would promote extensive synthesis of G-rich strands at the chromosome ends. This model would be most fitting for explaining ALT mechanisms (Cesare and Reddel, 2010).

II. Material and methods

Plasmids, siRNA, antibodies

The plasmid used for telomere probe generation (pSXneo270T_2AG_3) was a gift of Titia DeLange (Rockefeller University, USA). siRNA for *BRCA2* (GAA GAA CAA UAU CCU ACU ATT) or *GFP* (GUU CAG CGU GUC CGG CGA GTT) were made from Samchully Pharmaceutical company (Seoul, Korea). The following antibodies were purchased: anti-Actin (Santa Cruz; AC-15); anti-ATR (Santa Cruz; N-19); anti-TRF1(Abcam; ab1423); anti-TRF2 (NOVUS; NB100-2577).

Generation of MEFs and Cell culture

Brca2-conditional Knockout mice (*Brca2*^{f11}) were a gift from Dr. Anton Berns (NCI, The Netherlands). The MEFs were isolated from E13.5 embryos, cultured in DMEM supplemented with 15% FBS in 5% CO_2 humidified incubator. Cre recombinase was introduced with 100 MOI of *Cre*-expressing adenovirus. *GFP*-expressing adenovirus (Newgex, Korea) was introduced as a control.

Generation of polyclonal antibodies specific for Brca2

The sheep polyclonal antibodies specific to mouse Brca2 were generated by the injection of the recombinant mouse Brca2 protein, corresponding to 3,107-3,303 amino acids, purified from *E.coli* (National Blood Transfusion Service, UK). The rabbit polyclonal antibodies specific to human BRCA2 were generated by the injection of the peptide, corresponding to 1,382-1,395 amino acids of human BRCA2 (Peptron, Korea).

Telomere FISH

MEFs were incubated with 0.1 mg/ml colcemid (Sigma) for 4 hr at 37 °C, fixed in methanol/acetic acid (3:1) and processed for metaphase chromosome spread. When required, 0.2 μM of aphidicolin was treated for 16 hr, before cells were subjected to colcemid treatment. Chromosomes were stained using Cy3-OO-$(CCCTAA)_3$ PNA probe (Panagene, Korea) and DAPI. Fluorescent microscopy images were acquired using a CoolSnap HQ cooled CCD camera on a DeltaVision Spectris Restoration microscope built around an Olympus IX70 stand with a 60X/1.4 NA lens (AppliedPrecision).

Quantitative-FISH analysis

Quantitative-FISH (Q-FISH) on chromosome metaphase spreads were performed as described above (Poon and Lansdorp, 2001), in a blinded fashion. Metaphase spreads from MEFs were hybridized with Cy3-OO-$(CCCTAA)_3$ PNA probe and images were acquired using CoolSnap HQ cooled CCD camera on a DeltaVision. Telomere fluorescence intensity was analyzed using TFL-Telo software (gift from Peter Lansdorp, University of British Columbia, Canada).

Analysis of Anaphase bridges

Unsynchronized MEFs were grown on coverslips and fixed with 4% paraformaldehyde in PBS. DNA was counterstained with DAPI. Two experiments were performed independently and scored in a blinded manner. Images were acquired using axiocam MRm camera on Zeiss Observer Z1 inverted microscope with 40X/0.6 NA lens (Zeiss, Germany).

Analysis of Single stranded telomeric DNA

The amount of telomeric single stranded DNAs was assessed through hybridization in a non-denaturing condition. Assays used to determine the

replicative single G strand were followed from the protocol (Arnoult et al., 2009). Forty-eight hours after *Ad-Cre* infection, MEFs were synchronized in S-phase by treating 1.4 μM of aphidicolin for 12 hr (Dimitrova and Gilbert, 2000). Then, the cells were released into fresh medium with/without 5 mM of hydroxyurea. Genomic DNA were extracted using G-spin kit (Intron biotechnology, Korea), incubated overnight at 50℃ with [γ-^{32}P]-labeled telomeric C-rich probe [$(CCCTAA)_6$] in a hybridization buffer (50 mM NaCl, 10 mM Tris HCl [pH 8.0], 1 mM EDTA). Unbound free probes were separated by electrophoresis. Images were obtained by exposure to FLA3000 (FUJIFILM corporation) and normalized with ethidium bromide staining.

Telomere oligonucleotide ligation assay (T-OLA)

The telomere oligonucleotide assay (T-OLA) analysis was performed as described (Cimino-Reale et al., 2003; Cimino-Reale et al., 2001). Briefly, 24 hours after *Ad-Cre* infection, *Brca2*$^{f11/f11}$ MEFs were synchronized at G1/S by thymidine-aphidicolin block (Dimitrova and Gilbert, 2000). Cells were then released to S phase by changing to fresh medium for 4 h. 3 μg of genomic DNA was hybridized with a 0.5 pmol of [γ-^{32}P]-end-labeled nucleotide of the sequence $[(CCCTAA)_4]$ or $[(TTAGGG)_4]$. Hybridization was performed overnight at 50 °C, followed by ligation with 20 U of *Taq* DNA ligase (New England Biolab, USA) at 50 °C for 5 h. Then the samples were precipitated,

resuspended, and denatured in a formamide loading buffer. The samples were separated on 6 % acrylamide-6 M urea gels. Images were obtained by exposure to FLA7000 (FUJIFILM). 10 ng of T-OLA product was used for the quantitative PCR reaction of the genomic *GAPDH* gene for loading control.

Telomere-ChIP and Cell cycle analysis

HeLa_CFLAP-BRCA2_hTert was generated using retroviral vector pBabe_hTert into HeLa_CFLAP-BRCA2 cells (generous gift from Petronczki M. (Clare Hall laboratories, UK))**.** HeLa_CFLAP-BRCA2_hTert cells were subjected to double thymidine block to synchronize the cells in G1/S phase. Then the cells were released into fresh medium and collected at the indicated time points. Caffeine (2mM), Wortmannin (20μM or 200μM), KU55933 (20 μM) or CGK733 (20 μM), the drugs were added for 1 h before cell lysis. ATM, and ATR knock-down experiment were performed as described (Choi et al., 2009), cell lysis were performed 24 h post siRNA transfection. Telomere-ChIP assays were performed as described (Rizzo et al., 2009)

For BrdU incorporation experiment, HeLa cells were transfected with siRNAs for *BRCA2* or *GFP* were incubated with 20 mM BrdU (Sigma) for 30 minutes. Telomere-ChIP assay was performed as described (Rizzo et al., 2009) with the indicated antibodies. FACS analysis was performed as described (Darzynkiewicz and Juan, 2001)

C. elegans and RNAi feeding assay

trt-1(ok410) were grown on RNAi expressing lawns of HT115 (DE3) bacteria provided by Dr. Julie Ahringer (Wellcome Trust/ Cancer Research UK Gurdon Institute, University of Cambridge, UK). 20 worms at the L3 or L4 stage were picked from NGM agar plates containing 1mM IPTG and 50μg/mL ampicillin and transferred at 20 °C.

STELA (Single TElomere Length Analysis)

Measuring telomere length of V chromosome-Left arm was carried out as described. Worms were lysed for 1hr at 50 °C in Worm lysis buffer (100mM Tris 8.5, 100mM NaCl, 50mM EDTA, 1% SDS, 1% β-mercaptoethanol, 100 μg/ml Proteinase K). DNAs were purified by phenol/chloroform extraction and isopropanol precipitation. DNAs were treated with 2mg/ml RNase for 2hr After that Mbo1/Alu1 digestion were performed o/n. Phenol-chloroform extraction repeated once, and DNAs were diluted to a 20ng/μl concentration. A mixture of 20ng of DNA and 1μl of 10μM telorette was incubated at 60 °C for 10 min. Ligation was carried out using T4 ligase (NEB). Ligation reaction was inactivated by incubating 70 °C for 15 min. Ligated DNA was used as template for PCR. 94 °C for 3 min, 25 cycles of 94 °C for 20 sec, 64 °C for 30 sec, and

70 °C for 8 min, followed by final elongation at 70 °C for 10 min. PCR product were separated on 1% agarose gel. In gel hybridization was performed using as probe a ^{32}P-(TTAGGC)$_4$. Images were obtained by exposure to FLA7000 (FUJIFILM corporation).

C-, G-circle assay

Genomic DNAs was prepared as described above and digested with Alu1 and Mbo1. C-, G-circle assay was performed as described (Henson et al., 2009). DNAs were combined with 0.1mg/ml BSA, 0.5 mM dNTP and 1x ϕ 29 buffer with or without 7.5U ϕ 29 DNA polymerase, followed by incubation at 30 °C for 8 h and 65 °C for 20 min. Reaction products were dot-blotted then hybridized under native condition.

III. Results

III.1 Dysfunctional telomeres in the absence of BRCA2

III-1-1. BRCA2-deficient cells show end chromosomal fusion and signal free ends.

To elucidate the function of BRCA2 in telomere, I used embryo fibroblasts (MEFs) derived from Brca2 conditional knockout mouse (*Brca2*$^{f11/f11}$) **(FIGURE 9A)**. After introduction of Ad-Cre recombinase, intact Brca2 protein band disappeared in *Brca2*$^{f11/f11}$ MEFs (Jonkers et al., 2001) **(FIGURE 9B)**.

I performed Telomere-FISH on Brca2-deficient MEFs 5 days after infection to inspect dysfunctional telomeres in BRCA2-lacking cells. Depletion of BRCA2 showed telomere fusion phenotype **(FIGURE 9C)**. Both chromosomal fusions and chromatid fusions were increased in Brca2-deficient cells **(FIGURE 10A)**. The frequency of telomere signal-free ends (telomeres without detectable telomere repeats by T-FISH) was increased in Brca2-deficient cells **(FIGURE 10B)**.

As critically shortened telomeres can induce exchanges between leading and lagging strand telomeres through recombination, the incidence of telomere sister chromatid exchange (T-SCE) (Morrish and Greider, 2009; Wang et al., 2005) was measured by CO-FISH. The result showed that the absence of Brca2 provoked aberrant recombination (T-SCE at 1.67% incidence per chromosome), while the control MEFs barely showed any T-SCE **(FIGURE 10C)**.

Furthermore, critically shortened telomeres are also prone to be recognized as DNA double strand breaks (DSB), I can anticipate that significantly shortened telomere, shown as telomere signal-free end, might give a rise to end chromosomal fusions. In order to check another end chromosomal fusion phenotype, I analyzed anaphase bridges in BRCA2-deficient cells, the hallmark of end to end fusion (Gilson and Geli, 2007). Anaphase bridge formations were increased up to 37% in Brca2-deficient MEFs **(FIGURE 10D)**.

As anaphase bridges lead to breakage-fusion-bridge (BFB) cycle, these events are partially responsible for accumulated chromosomal aberration in BRCA2-deficient cells. The observed fusion phenotypes are derived primarily from dysfunctional telomere, distinct from gross chromosomal rearrangement phenotype in Brca2-deficient cells (Yu et al., 2000). Altogether, the increase

of end-to-end fusions and telomere signal-free ends, and anaphase bridges in Brca2-deficient cells demonstrate that dysfunctional telomeres arise in the BRCA2 absent condition.

Figure 9.

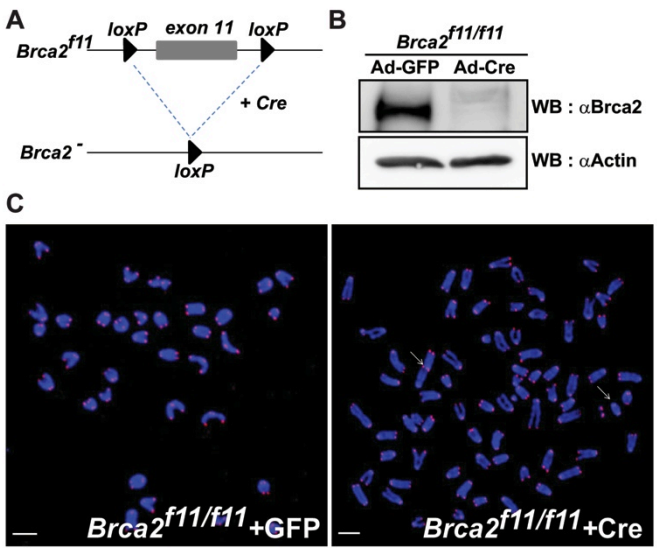

Figure 9 End-to-end fusions arose in Brca2-deficient MEFs

Figure 9. End-to-end fusions arose in Brca2-deficient MEFs.

A. Illustration of *Brca2*^{f11} alleles using the Cre-loxP system. LoxP sequences are inserted at intron 10 and intron 11 for floxing exon 11.

B. Western blot (WB) to analyze the efficiency of Cre recombinase after Ad-Cre infection in *Brca2*$^{f11/f11}$ MEFs. Brca2 disappears when *Ad-Cre* is expressed. Same blot was re-probed with anti-Actin antibodies for normalization.

C. *Brca2*$^{f11/f11}$ MEFs were either infected with Ad-GFP or Ad-Cre. Five days post infections, MEFs were subjected to telomere FISH analysis. At least 15 metaphases from two independent MEFs from the same siblings were analyzed. Representative image of telomere FISH in *Brca2*$^{f11/f11}$ MEFs infected with Ad-GFP or Ad-Cre are shown. Arrows depict chromosomes with end-to-end fusion or chromatid fusion. Scale bars, 5 mM

Figure 10.

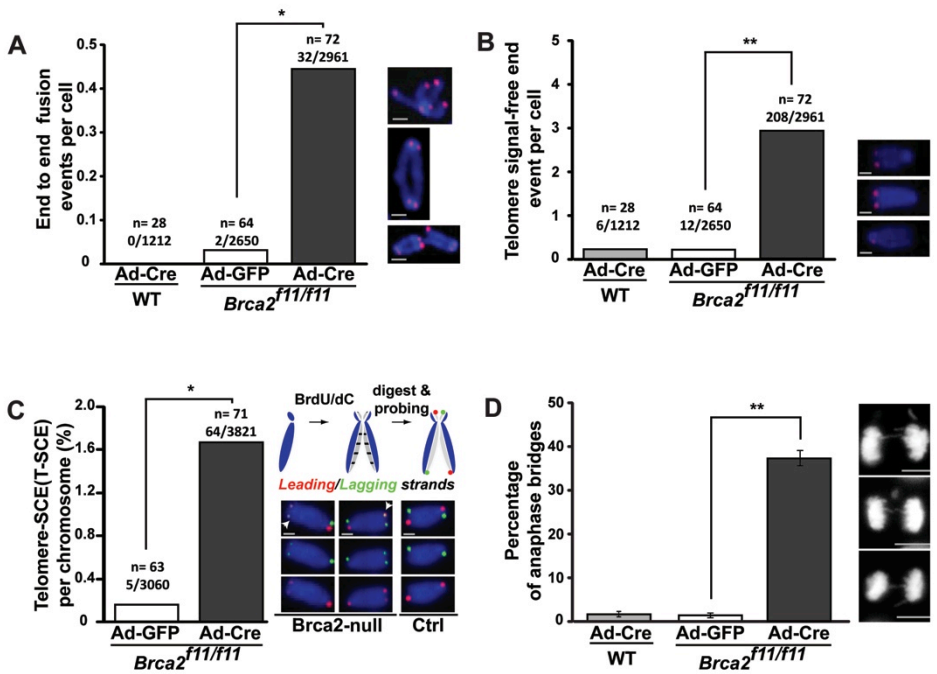

Figure 10 Dysfunctional telomeres in Brca2-deficient MEFs

Figure 10. Dysfunctional telomeres in Brca2-deficient MEFs

A. The frequency of telomere end-to-end fusion events. Each chromosomes were closely examined for any telomere fusions. Bar graphs indicate the frequency of telomere fusions in all of the chromosomes analyzed x/y, Total number of chromosomes with end-end fusion/Number of cells analyzed; n, number of all chromosome analyzed. Enlarged images are shown at the right. Scale bars, 1 mm.

B. The frequency of telomere signal-free end events. Bar graphs indicate the frequency of telomere signal-free ends in all of the chromosomes analyzed x/y, Total number of chromosomes with telomere signal-free ends/Number of cells analyzed; n, number of all chromosome analyzed. Representative images are shown at the right. Scale bars, 1 mm.

C. T-SCE measured in the presence (Ad-GFP) or absence (Ad-Cre) of Brca2. CO-FISH assay was performed 5 days post adenoviral infection. Wild-type cells display lagging (green) and the leading (red) strand in a diagonal orientation in control (schematic diagram above, see also Experimental Procedures). Leading and/or the lagging strand appearing in the non-diagonal orientation are judged to result from the telomere sister chromatid exchanges, and was observed in Brca2-null MEFs. T-SCEs are marked with while arrows. The results are from three independent experiments. x/y, Total number of T-SCEs/number of chromosomes analyzed; n, number of cells analyzed. Representative images are shown at right.

D. Quantification of anaphase bridges after *Cre* expression in $Brca2^{f11/f11}$ MEFs or wild type MEFs. Bar graphs indicate the percentage of cells displaying anaphase bridges 5 days post adenoviral infection. At least 63 cells in anaphase were analyzed. Scale bars, 5 mm.

[*: $P<0.05$, **: $P<0.01$,; T-test]

III-1-2. BRCA2-deficient cells induce telomere length rapid deletion.

Since chromosomal end fusions and telomere signal-free ends can result from shortening of telomere, I measured telomere lengths by using Quantitative-FISH (Q-FISH) in MEFs metaphase spreads. After Brca2 depletion, by infecting *Ad-Cre*, I examined telomere lengths 2 days and 7 days post-infection. I found that the mean length of Brca2-deleted MEFs telomeres was ~ 25% shorter than that of Control MEFs **(FIGURE 11)**. These data suggest that critically shortened telomeres in Brca2-deficient cells resulted in end-to-end fusions and telomere signal-free ends.

Figure 11.

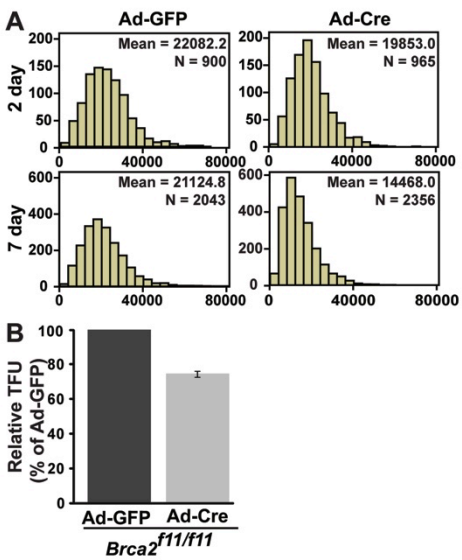

Figure 11 Telomere length Rapid Deletion (TRD) in Brca2-deficient MEFs

Figure 11. Telomere length Rapid Deletion (TRD) in Brca2-deficient MEFs

Brca2$^{f11/f11}$ MEFs were analyzed for their overall telomere length at day 2 and day 7 after infection with Ad-Cre or Ad-GFP by measuring the fluorescent telomere signals with Q-FISH (TFL-Telo program, gift from Peter Lansdorp, University of British Columbia, Canada)

A. Relative intensity of the telomere signals in *Ad-Cre*-infected MEFs, compared to those of control *Ad-GFP*-infected MEFs. Chromosomes from at least 60 different cells each were analyzed. Bars represent the relative fluorescence intensity over control cells (Ad-GFP), measured at day 7 post viral infection in *Brca2*$^{f11/f11}$ MEFs.

B. Telomeres shorten in Brca2-deficient MEFs in a passage-dependent manner. *Ad-Cre* infected *Brca2*$^{f11/f11}$ MEFs display a significantly increased degree of telomere shortening after Ad-Cre expression, compared to control (Ad-Cre). X-axis, relative fluorescence units; Y-axis, number of chromosomes; N, number of chromosomes analyzed. Mean value of relative fluorescence units are also indicated. Data were analyzed using SPSS software.

III-1-3. Telomere erosion induced DNA damage response in the absence of BRCA2

Telomeric dysfunctions converge with DNA damage sites; therefore telomere dysfunction-induced foci (TIFs) have been detected in cells with telomere erosions (Takai et al., 2003). To analysis if Brca2-deficient MEFs have accumulated TIFs, I performed immune-FISH, using the anti-53BP1 antibody, as 53BP1 is a marker for DSB (Wang et al., 2002). The TIFs were 4 to 5 fold higher when BRCA2 is absent compared to control cells **(FIGURE 12)**. This indicates that telomere damage responses are more frequently generated in BRCA2-deficient conditions, which might be partially due to the excessive loss of telomeric DNA lead to induction of DNA damage response at telomere. In the absent of BRCA2, elevated DNA damage responses in telomere would bring NHEJ prone condition between chromosomal ends.

Figure 12.

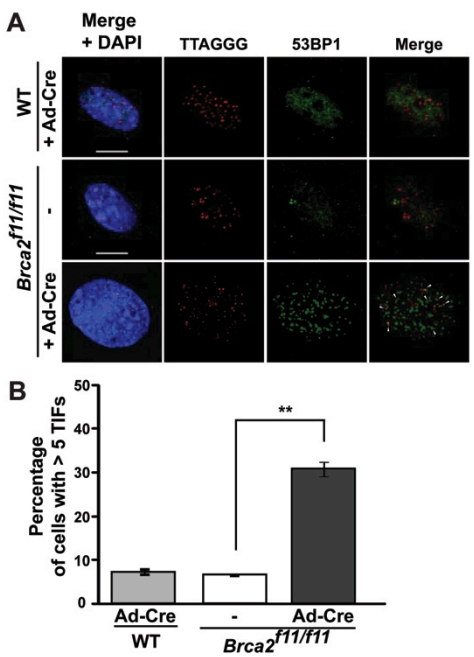

Figure 12 Increased Telomere dysfunctional induced foci (TIFs) in Brca2-null MEFs

Figure 12. Increased Telomere dysfunctional induced foci (TIFs) in Brca2-null MEFs.

A. Represented cells illustrated telomere dysfunction induced foci (TIFs) analysis using 53BP1 anti-serum and telomere probe in *Brca2*$^{f11/f11}$ MEFs or wild type MEFs, either infected with Ad-GFP or Ad-Cre at day 5 after viral infection.

B. Quantification of the TIF analysis as shown in (A). Bar graphs indicate the percentage of cells with more than 5 TIFs. Scale bars, 5 mm. [**: P<0.01, T-test]

III-2. BRCA2 is required for the telomere replication homeostasis

III-2-1. BRCA2 localizes to the telomeres during DNA replication in an ATR-dependent manner.

To verify the roles of BRCA2 at the telomere, I performed telomere chromatin immunoprecipitation (Telomere-ChIP) assay in HeLa_CFLAP-BRCA2_hTERT cells (expressing Flag-tagged BRCA2 in endogenous level) using α-Flag antibody (M2). Since Telomere-ChIP against BRCA2 using short telomere contained cells (IMR90 or HeLa) did not work well (Data from our group, unpublished Data), we used HeLa_CFLAP_BRCA2_hTERT cells, which is generated by introducing hTERT-expressing retrovirus into HeLa_CFLAP_BRCA2. The hTERT overexpression in HeLa cells generates 4 to 5 fold longer telomere than normal HeLa cells. Cells were synchronized by double thymidine block, and released into fresh medium and collected at the indicated time points **(FIGURE 13C)**. Telomere-ChIP assay results revealed that localization of BRCA2 in telomere is abundant and peaked at S phase **(FIGURE 13A, B)**. Thus BRCA2 has an ability to associate with telomeres, dominantly at S phase. It is similar disposition to previous report that DNA repair proteins are localized at the telomere during replication (Verdun and

Karlseder, 2006). Since HeLa_CFLAP_hTERT cells contained artificially engineered long telomeres, the amount of precipitated telomere DNA in HeLa_CFLAP_BRCA2_hTERT cells (**FIGURE 13B**) would not represent the physiological amount of BRCA2 at the telomeres.

PI3K family proteins such as ATM and ATR are the major sensors of DNA damage. Moreover, telomere function depends on checkpoint proteins such as ATM and ATR (Verdun and Karlseder, 2006). To investigate the possibility that ATM/ATR pathways are responsible for the function of BRCA2 at the telomere, I tested whether the localization of BRCA2 at the telomere during replication is ATM/ATR-pathway dependent by using inhibitors of these pathways. It is reported that caffeine and wortmannin can inhibit activity of both ATM and ATR, but the dose 2mM caffeine or 20μM wortmannin that preferentially inhibit ATM pathway in vivo. In dose of 200μM wortmannin, ATR pathway is also completely inhibited. Moreover, various ATM, ATR specific inhibitors, such as KU55933 (ATM inhibitor) and CGK733 (ATM and ATR inhibitor), has been developed recently. Four hours after release, the time when cells are enriched in S phase **(FIGURE 13C)**, cells were challenged with Caffeine, Wortmannin, CGK733 or KU55933 for 1 h. Localization of BRCA2 at the telomere was dramatically reduced when 200μM of wortmannin (~48%) or 20μM of CGK733 (~68%) were treated, not much

when 2mM of caffeine, 20μM of wortmannin, or 20mM of KU55933 were treated **(FIGURE 14A-D)**.

Encountering off-target effects of inhibitors and arguing for target specificity, HeLa_CFLAP-BRCA2_hTert cells were transfected with siRNAs against ATM or ATR, and then telomere-ChIP were performed. When siATR was transfected, localization of BRCA2 at the telomere was reduced (~60%), whereas *ATM* knockdown (siATM) had no effect **(FIGURE 14E-G)**, confirming that BRCA2 localization at the telomeres requires ATR. I can conclude that ATR-pathway is responsible for localization of BRCA2 at the telomere during replication.

Figure 13.

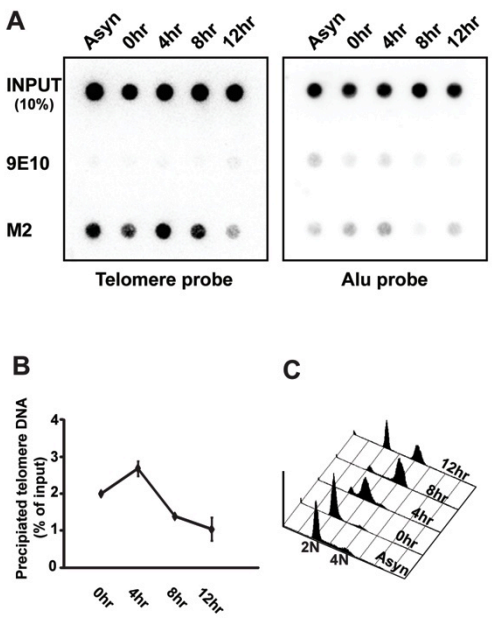

Figure 13 BRCA2 localized at the telomere during S phase

Figure 13. BRCA2 localized at the telomere during S-phase

A. HeLa_CFLAP-BRCA2_hTert cells were synchronized at the telomere by double thymidine block then released into the cell cycle. Cell lysates were prepared at the indicated time point from thymidine release and subjected to telomere ChIP assay.

B. The percentage of precipitated telomere DNA was measured as a ratio of input signals and marked as dotted graphs at each time points. Note the maximum dot intensity in 4hr time point from double thymidine block and release, which represent S phase cells (C).

C. Cell cycle profiles of each time points are measured using FACS analysis. Cell cycle profiles are not influenced by BRCA2 knockdown.

Figure 14.

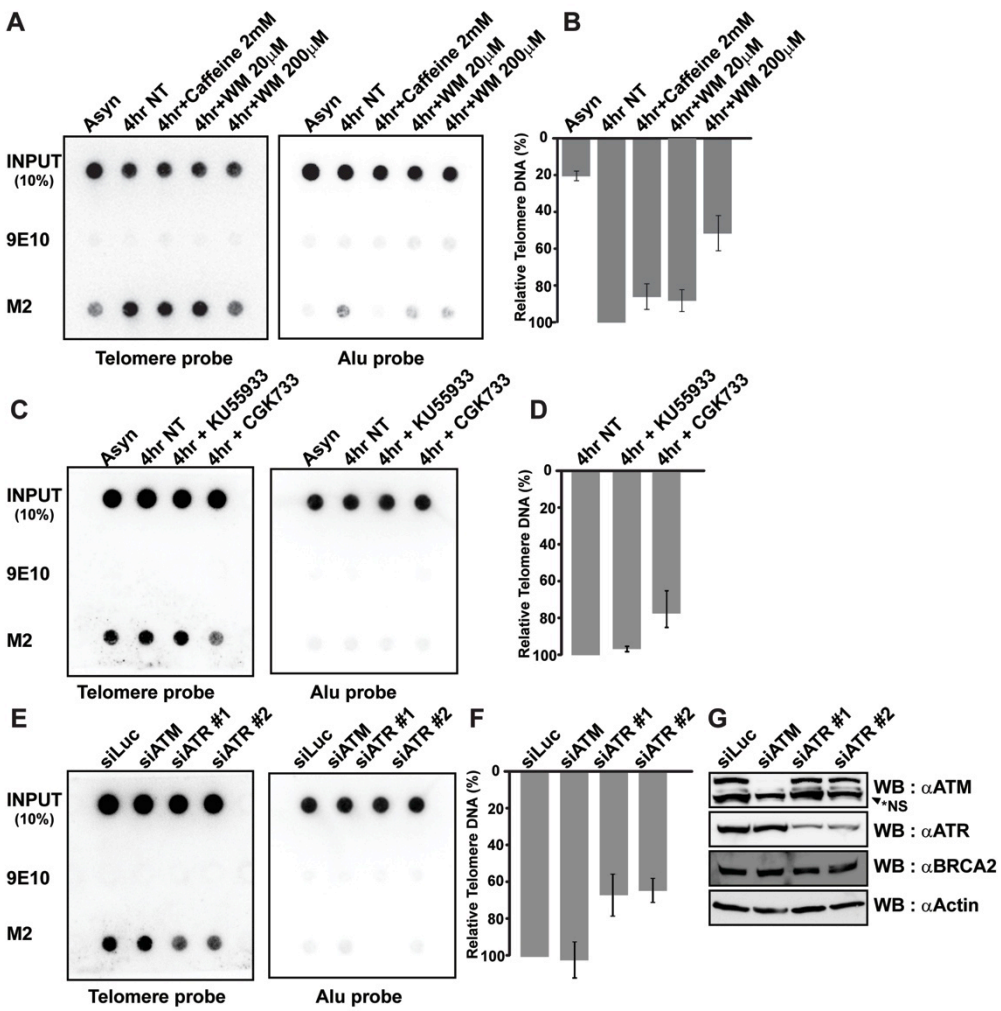

Figure 14 BRCA2 localized at telomere in an ATR pathway dependent manner

Figure 14. BRCA2 localized at telomere in an ATR-pathway dependent manner.

A, C. HeLa_CFLAP-BRCA2_hTert cells were treated or not treated caffeine (2mM), wortmannin (2mM (ATM inhibition) or 200mM (ATM and ATR inhibition)), KU55933 (20mM, ATM specific inhibitor), or CGK733 (20mM, ATM and ATR inhibitor) for 1hr after 4hr from thymidine release. Lysates were also performed telomere ChIP.

B, D. Bars represent the relative telomere DNA measured from the densitometer. The signals were normalized with input. Note the significant decrease of dot intensity, in response to wortmannin 200mM or CGK733 20mM treatments.

E. HeLa_CFLAP-BRCA2_hTert cells transfected with indicated siRNAs. Cell lysates were prepared 24 h post transfection. Telomere ChIP assay was performed with anti-FLAG (M2, BRCA2) and 9E10.

F. Western blot analysis to assess the efficiency of siRNAs employed in the assay in E and F.

III-2-2. BRCA2-deficient cells exhibit telomere fragility resulting from problems in lagging strand synthesis.

Telomere repeats pose a challenge in DNA replication, for it will be subjected to defects in replication process (Gilson and Geli, 2007). I focused on telomere replication problem that could be related with dysfunctional telomere phenotype in Brca2-deficient MEFs and the function of BRCA2 at the telomere during S phase. In order to inspect this speculation, first of all, I analyzed the forms of telomere signals in metaphase-spread chromosomes under BRCA2-lacking condition to evaluate fragile telomeres. Brca2-deficient cells showed increased fragile telomere phenotype, such as broken telomeric signals, failed condensation signals or multiple telomeric signals (MTS) **(FIGURE 15A, right)**. Comparable results were observed in BLM- or RTEL-deficient telomere (Sfeir et al., 2009). Fragile telomeres were increased in aphidicolin (DNA polymerase α inhibitor)-treated wild type and *Brca2* null MEFs **(FIGURE 15A, B)**. This gain of fragile telomere primarily demonstrates the DNA replication defects in telomere. ATR knock down also enhanced the fragile-telomere phenotype of Brca2-deficient cells **(FIGURE 15C, D)**, which is known as replication-related checkpoint protein and ATR deficiency also induce fragile telomere expression (McNees et al., 2010; Pennarun et al., 2010). Enhanced fragile telomere expression in ATR inhibited-Brca2-deficient cells would be resulted from blocking of alternative protection pathway for Brca2-deficient condition, which is regulated by ATR.

Telomeric Parental lagging strands are prone to trouble during replication in the absence of WRN, a G-quadruplex helicase. WRN deficient cells exhibit lagging strand specific deletion (Crabbe et al., 2007). It has been also reported that DNA repeat on the lagging-strand template can adopt unusual DNA structures when it becomes single stranded in a region between okazaki fragments during DNA replication, causing preferential instability of repeats on the lagging strand (Rosche et al., 1995; Trinh and Sinden, 1991). To test if telomeric replication problem has strand specificity, I asked whether fragile telomeres induced by Brca2 depletion display strand preference. By using Chromosome Orientation-FISH (CO-FISH) which enables distinguish parental lagging strand (G-rich, green) from parental leading strand (C-rich, red). Even in control MEFs, treatment with 0.2 mM Aph led to the increase of lagging strand-specific fragile telomere (~8%; **FIGURE 16B**), which indicates that G-rich parental lagging strands are more susceptible to expressing fragile sites. Treatment of Aph in Brca2-deficient MEFs further increased the G-rich lagging strand telomere fragility (~13%; **FIGURE 16B**). Moreover, T-SCEs were increased in Aph treated MEFs (**FIGURE 16D**). And, T-SCE in Brca2-deficient MEFs was increased upon Aph treatment (~7.3%; **FIGURE 16D**), suggesting that the replication problems in G-rich parental lagging strand telomeres would be linked to the marked increase of T-SCE in Brca2-deficient MEFs.

Figure 15.

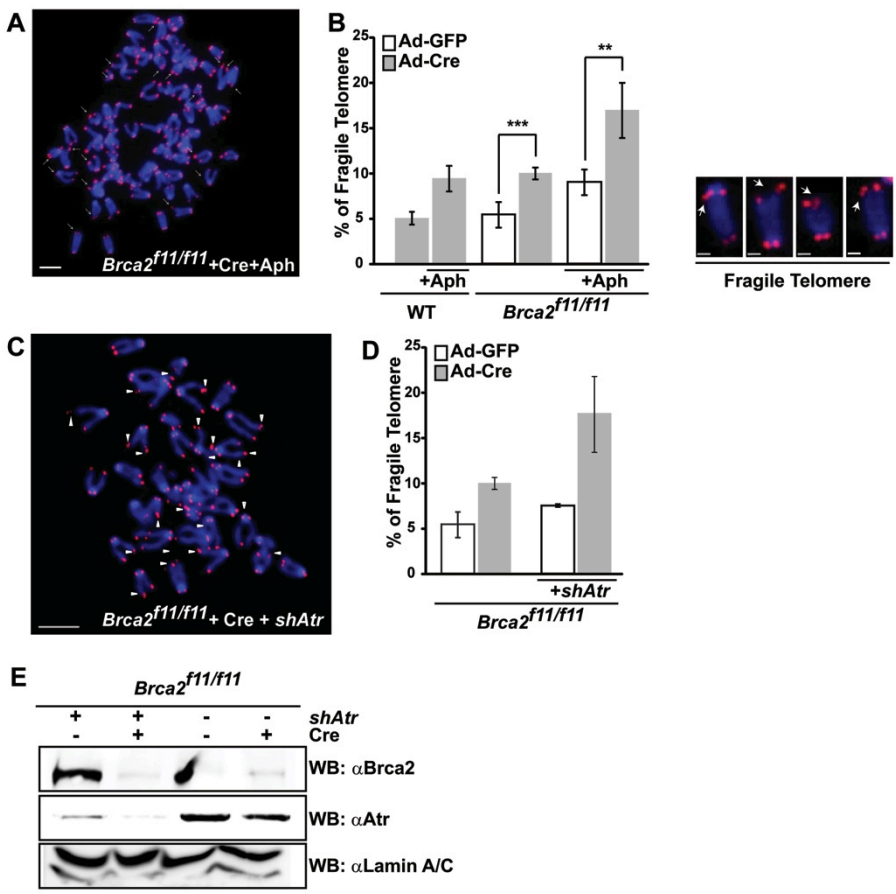

Figure 15 Brca2-deficient MEFs exhibit fragile telomeres

Figure 15. Brca2-deficient MEFs exhibit fragile telomeres.

A, C. Brca2-deficient cells exhibit fragile telomeres. *Brca2*$^{f11/f11}$ MEFs were subjected to Telomere FISH after Ad-Cre infection and aphidicolin (Aph) treatment (A) or Atr depletion (C). Image is from one representative telomere-FISH. Arrowhead depicts the chromosomes with telomere fragility. Bars, 5 mm

B. *Brca2*$^{f11/f11}$ MEFs or wild type MEFs were treated with 0.2 mM of aphidicolin (Aph) and analyzed for fragile telomeres. Note the significant increase of fragile telomeres following Ad-Cre infection, in response to Aph treatment (+Aph). Bars represent the percentage of fragile telomeres in total number of chromosomes analyzed 5 days post adenoviral infection. Representative images are shown at the right. Bars, 1 mm

D. *Brca2*$^{f11/f11}$ MEFs were treated with lenti-viral shAtr and analyzed for fragile telomeres. Note the significant increase of fragile telomeres following Ad-Cre infection, in response to depletion of *Atr* (shAtr). Bars represent the percentage of fragile telomeres in total number of chromosomes analyzed 5 days post adeno-viral and lenti-viral infection.

E. WB showing the efficiency of Brca2 and/or ATR depletion after viral infection. Same blot was reprobed with anti-Lamin A/C for normalization.

[**: P<0.01, ***: P<0.001; T-test]

Figure 16.

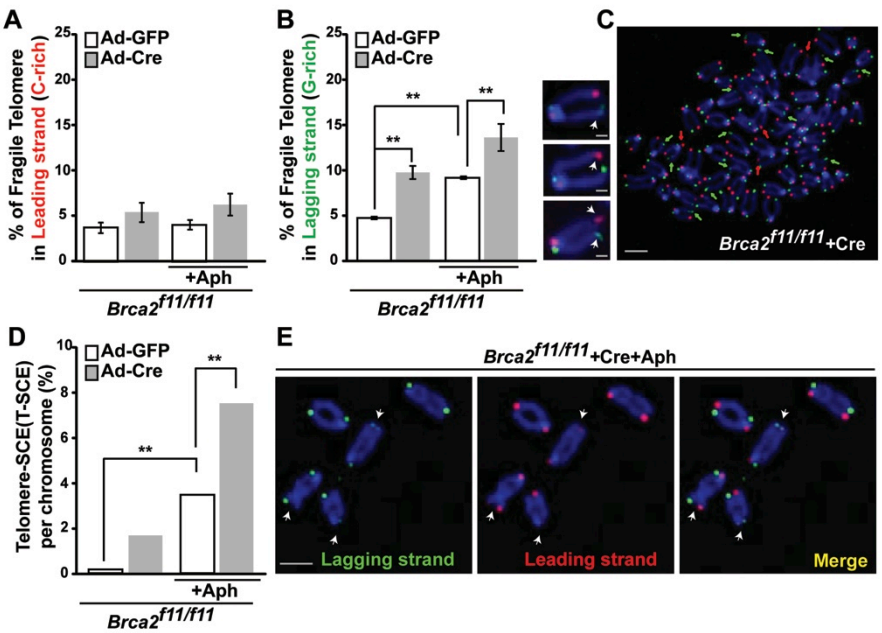

Figure 16 BRCA2-deficient cells exhibits telomere fragility result from lagging strand synthesis problems

Figure 16. BRCA2-deficient cells exhibit telomere fragility result from lagging strand synthesis problems.

Comparison of fragile telomeres in leading and lagging strands after Brca2 depletion

A, B. *Brca2*$^{f11/f11}$ MEFs infected with *Ad-GFP* or *Ad-Cre* were subjected to CO-FISH after Aph treatment. Bars represent the percentage of fragile telomeres in leading or lagging strand, analyzed 2.5 days post-adenoviral infection. Representative images of telomere fragility are shown at the right. Scale bar, 1 μm.

C. Telomere fragility in lagging strands is higher compared to the leading strand in Brca2-deficient MEFs. Green arrowheads, fragile telomeres in lagging strand. Red arrowhead, fragile telomeres in leading strand. Scale bar, 5 μm.

D. T-SCE measured in the presence (Ad-GFP) or absence (Ad-Cre) of Brca2 with/without Aph treatment.

E. Brca2-deficient MEFs treated with Aph display a marked increase in T-SCE. Note the arrowheads, which indicate T-SCE. Scale bar, 5 μm.

III-2-3. Accumulation of G-rich single-stranded telomeres during replication in Brca2-deficient cells

Single stranded DNA accumulates in telomeres during S phase by replication uncoupling or breakdown of the replication forks (Arnoult et al., 2009). Therefore, I asked whether single stranded DNA accumulate in telomeres of Brca2-deficient cells. Single-stranded telomeric DNA analysis assay was performed under BRCA2-deficient condition to examine the phenotype that has arisen due to replication defect. The amount of G-rich single stranded telomeric DNA increased in Brca2-deficient cells. This increase in amount of G-rich single stranded telomeric DNA in Brca2-deficient cells dramatically swelled under hydroxyurea (HU) treated condition **(FIGURE 17)**. Since HU treatment causes depletion of dNTPs, DNA replication forks are stalled and progressively inactivated (Petermann et al., 2010). In absence of BRCA2, single stranded telomeric DNA dramatically increased in response to HU, indicating that stalled replication forks cannot be protected. I can assume that frequent occurrence of stalled fork affects G-rich single stranded DNA accumulation at the telomeres of BRCA2-null cells. Hence, telomeres in Brca2-deficient cells display single stranded telomeric DNA accumulation during replication, which results from defects in protection of stalled replication fork.

Figure 17.

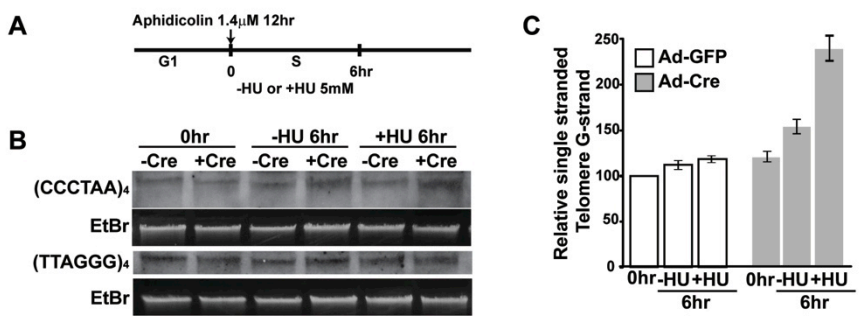

Figure 17 Single stranded telomere DNAs are accumulated in Brca2-lacking conditions

Figure 17. Single stranded telomere DNAs are accumulated in Brca2-lacking conditions.

Generation of single stranded telomeres in response to hydroxyurea (HU) treatment was measured 2 days post adenoviral infection in *Brca2*$^{f11/f11}$ MEFs.

A. MEFs were synchronized in S phase by treating 1.4 mM aphidicolin for 12 hours, changed to fresh media and treated/untreated with 5 mM of HU for 6 hours.

B. Genomic DNA were hybridized with radiolabeled probes under denaturing condition. Probes specifically hybridizing to telomeric DNA were detected after gel migration.

C. Bars represent the relative single stranded G-rich strands measured from the densitometer. The signals were normalized with total DNA (Etbr, ethidium bromide).

To corroborate single stranded telomeric DNA assay result, the length of the single stranded DNA at the telomeres were measured and compared by telomere-oligonucleotide ligation assay (T-OLA) (Cimino-Reale et al., 2001; Stewart et al., 2003; Yang et al., 2005). The ligation product and signal intensity are the indications for the length and amount of telomeric overhangs and the single stranded telomeric DNA. Control MEFs and *Brca2*-deficient MEFs were blocked in G1/S phase and released 4 hour to collect S phase cells. The genomic DNAs were extracted from G1/S arrested and S phase cells and subjected to T-OLA analysis. After Ad-Cre infection 3 days, T-OLA assays were performed. G-rich tails were significantly longer than C-rich tails as previously reported (Cimino-Reale et al., 2001) ; Brca2-deficient MEFs displayed similar G-, or C-rich tails compared to control **(FIGURE 18A)**, which indicates that there is no overall overhang changes in this condition. I assessed the length and amount of G tails and C tails in G1/S and S phase, respectively, and compared them in the presence or absence of Brca2. Interestingly, G-rich tails increased to 2.5-fold in S phase of Brca2-depleted cells (**FIGURE 18B**, +Cre), while the control cells displayed 1.4-fold increase in S phase (**FIGURE 18B**, -Cre). These results indicate that Brca2-deficient cells exhibit G-rich single stranded DNA accumulation during S phase.

Related to this, a recent report has demonstrated that Rad51 and BRCA2 protect newly synthesized DNA from Mre11-dependent resection, which is

distinct from its function in HR (Hashimoto et al., 2010; Schlacher et al., 2011). Since my data suggest that telomere fragile site expression in Brca2-deficient cells is related to lagging strand (G-rich parental strand) problem **(FIGURE 16)**, it is possible that the increase of G-rich single stranded DNA in the absence of Brca2 is associated with the resection of nascent strand of the G-rich lagging strands during telomere replication **(FIGURE 20).**

Figure 18.

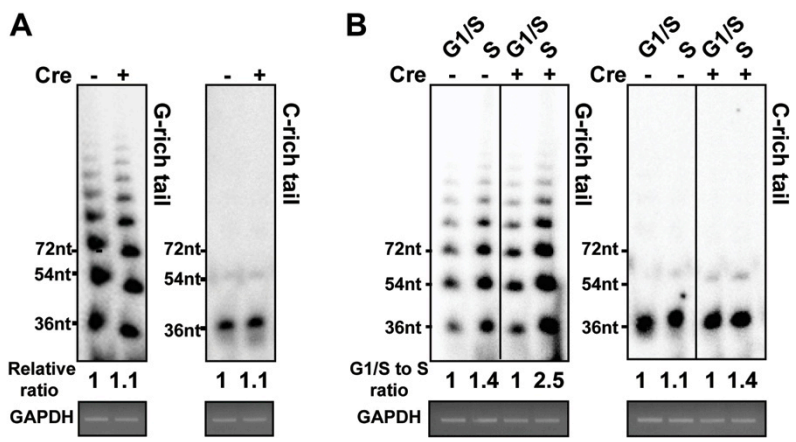

Figure 18 Accumulation of G-rich single stranded telomeres during replication in Brca2-deficient cells

Figure 18. Accumulation of G-rich single stranded telomeres during replication in Brca2-deficient cells

A. T-OLA analysis (Cimino-Reale et al., 2003) of *Brca2*$^{f11/f11}$ MEFs with oligonucleotides complementary to the G-rich tail $[CCCTAA]_3$, or the C-rich tail $[TTAGGG]_3$, 2.5 days post *Ad-GFP* (-Cre) or *Ad-Cre* (+Cre) infection. Relative hybridization intensity and length to the control are marked. GAPDH PCR product is shown for normalization of genomic DNA employed.

B. *Brca2*$^{f11/f11}$ MEFs infected with *Ad-GFP* or *Ad-Cre,* were synchronized in G1/S by thymidine-aphidicolin block, then released into S phase progression by incubating in fresh media for 4 h. T-OLA assay was performed 2.5 days post-adenoviral infection. Relative intensity and length of T-OLA product in each lane are marked: the intensity of T-OLA product in G1/S in each setting is set to 1. Note the significant increase of G-rich single stranded telomeric DNA following Ad-Cre infection during S-phase. PCR product of GAPDH is included for control. (**: $P<0.01$, ***: $P<0.001$; t-test).

III-2-4. Telomeric DNA replication fidelity is impaired in the BRCA2-lacking cells

Based on my observations, Brca2-deficient cells showed increase in fragile telomere, and single stranded G-rich telomeric DNA accumulated in S phase, I could anticipate that telomeric DNA replication fidelity is impaired in BRCA2-lacking condition. To estimate the effect of BRCA2-deficiency on telomere replication, I performed Telomere-ChIP assay in HeLa Cells, in which BrdU incorporation by 6 rounds of 30 min pulse and 2 h 30 min chase using anti-TRF1 and anti-TRF2 serum. Knock down of BRCA2 in HeLa cells resulted in reduced BrdU incorporation in telomere (~60%), which indicates reduced telomeric DNA replication efficiency, though it is not due to difference in cell cycle profile **(FIGURE 19)**.

Previous reports show that speeds of replication fork in BRCA2-null cells are slower than that of wild-type cells and this is overcome by narrowing replication origin distance (Daboussi et al., 2008). Since telomeres have limited numbers of replication origin, telomere replication is usually unidirectional (Gilson and Geli, 2007; Sfeir et al., 2009). In addition to defects of stalled fork protection in BRCA2-deficient cells, poor telomere replication efficiency in BRCA2-deficient cells was not able to overcome by modulating replication origin number.

Collectively, these data exhibit that BRCA2 is required for efficient and complete DNA replication process in telomere. I can also suggest that S phase is terminated without complete telomere replication under BRCA2 lacking condition as represented by dysfunctional telomeres.

Figure 19.

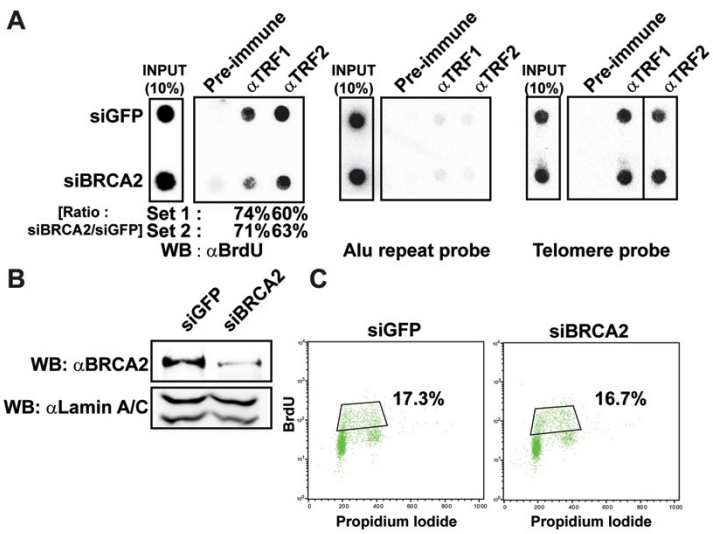

Figure 19 BRCA2 is required for enhancing the fidelity of telomere replication

Figure 19. BRCA2 is required for enhancing the fidelity of telomere replication

A. HeLa cells were transfected with siRNA for *GFP* (siGFP) or *BRCA2* (siBRCA2). They were then pulsed with BrdU for 30 min and chased for 2 h and 30 min. This cycle was repeated 6 times. Lysates were incubated with anti-TRF1 or –TRF2 antibodies and subjected to Telomere-ChIP. The blot was immunoblotted with anti-BrdU antibodies to assess the amount of replicated telomeric DNAs. Note the significant decrease of BrdU incorporation, in response to siBRCA2 treatment. ChIP assays were also performed with Alu or telomere probes to verify the efficiency of ChIP.

B. WB and FACS analysis of S-phase progression for BRCA2 knockdown in HeLa cells. The percentage of cells in S-phase is indicated in Graphs. Same blot was probed with anti-Lamin A/C for normalization.

Figure 20.

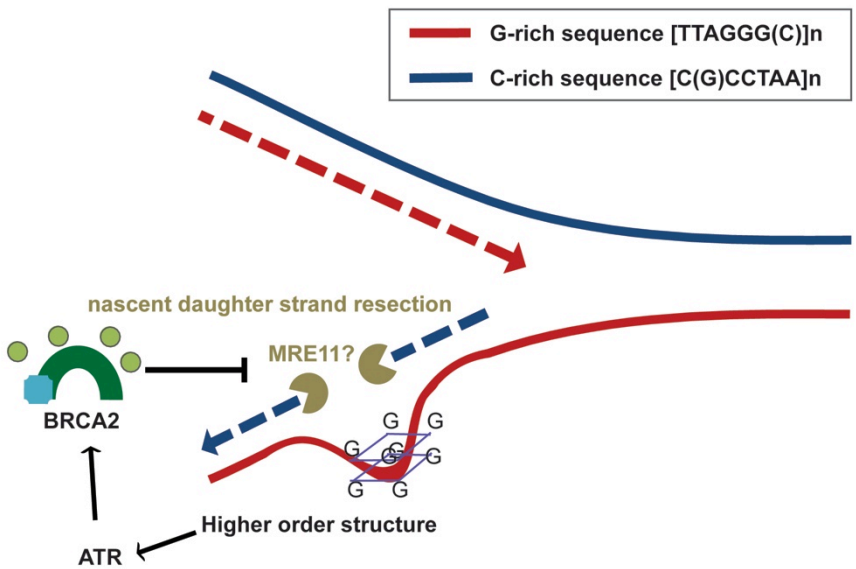

Figure 20 The proposed function of BRCA2 in the maintenance of telomere replication fidelity

Figure 20. The proposed function of BRCA2 in the maintenance of telomere replication fidelity

Telomere possesses G-rich strand as parental lagging strand, and C-rich strand as parental leading strand. Blockages would be formed more frequently at the lagging strands during DNA replication, since G-rich parental strands exposed as single strands between Okazaki fragments can adopt higher-order structures such as G-quadruplex. Since BRCA2 protects the nascent strand at stalled replication fork from MRE11-dependent resection, in the absence of BRCA2, the resection of daughter strands would be more frequent at lagging strands.

III-3. Induction of ALT-like phenotype in the absence of BRCA2

III-3-1. BRCA2 RNAi in telomerase-mutant worms induces extended propagation.

Cancer cells should acquire a mechanism to counteract progressive telomere length shortening that occurred as a result from end replication problem (Brault and Autexier, 2011). ALT (alternative lengthening of telomere) is the mechanism for cancer cells maintain their telomere lengths, independent from the reactivation of telomerase. In our group, we observed that the transformed MEFs from *Brca2*$^{Tr/Tr}$ (*Brca2Tr/Tr*-R273L, -G154V) displayed features of ALT. So I tested whether BRCA2 indeed suppresses ALT by using *C. elegans* model system, which is the best model organism for studying telomere biology as previously done (Im and Lee, 2005; Joeng et al., 2004; Park et al., 2010).

An orthologue of BRCA2, brc-2 is present in *C. elegans* (Martin et al., 2005). The function of *brc-2* in homologous recombination is evolutionary conserved (Min et al., 2007). Since *brc-2* mutant worms are sterile and lethal due to meiotic recombination failure, I could not use *brc-2* mutant for investigating

the function of BRCA2 in ALT, rather I used feeding RNAi system to target *brc-2* expression. Thus I tested whether *brc-2* RNAi in *trt-1 (ok410)* would trigger ALT phenotype. *trt-1* is a telomerase orthologue in *C. elegans. trt-1 (ok410)* showed telomere shortening through generations, hence the brood size was decreased and eventually become sterile (Meier et al., 2006).

trt-1(ok410) fed L4440 (empty vector, control) RNAi finished laying their progeny at 21th generation **(FIGURE 21B,** black **)**. *trt-1 (ok410)* fed *brc-2* RNAi delayed the mortal phenotype of *trt-1 (ok410)* and continued to lay progenies until 35th generation **(FIGURE 21B,** wine**)**. *rad-51* RNAi and *rad-54* RNAi also continued generation until ~35th, ~33th generation (**FIGURE 21B**, navy, emerald), which indicate that prolonged generation in *trt-1(ok410)* fed *brc-2* RNAi is associated with the deficiency of *brc-2* `s function in homologous recombination. RNAi of *pot-1*, a paralogue of POT-1, which binds to C-overhang, result in prolonged generation as previously reported (Lackner et al., 2012) (**FIGURE 21B**, violet).

Since *cep-1,* an orthologue of p53 in *C. elegans*, is responsible for apoptosis induction in meiotic germ cells in response to meiotic recombination failure, we fed *cep-1, brc-2* double RNAi to reduce apoptotic effects in germ cells which is result of meiotic recombination failure in *brc-2* RNAi. *trt-1 (ok410)* fed *cep-1* RNAi finished their generation at the similar stage to *L4440* (empty

vector, negative control) (**FIGURE 21C**, gray). *trt-1 (ok410)* fed *cep-1*; *brc-2* double RNAi and *cep-1*; *rad-51* double RNAi also finished their generation at the similar stage to *brc-2* and *rad-51* single RNAi (**FIGURE 21C**, navy, emerald), however, the survival rates were sustained and brood sizes does not decreased until the generation is not prolonged **(FIGURE 21C)**. This phenotype indicates that extended propagation in *trt-1(ok410)* fed *brc-2* RNAi is not originated from defects in meiotic recombination but ALT phenomena result from BRCA2-depletion. Furthermore, this result implies that inactivation of checkpoint would enhance the proliferative capacity, not affect on ALT phenotypes results from the BRCA2-deficient condition.

Figure 21.

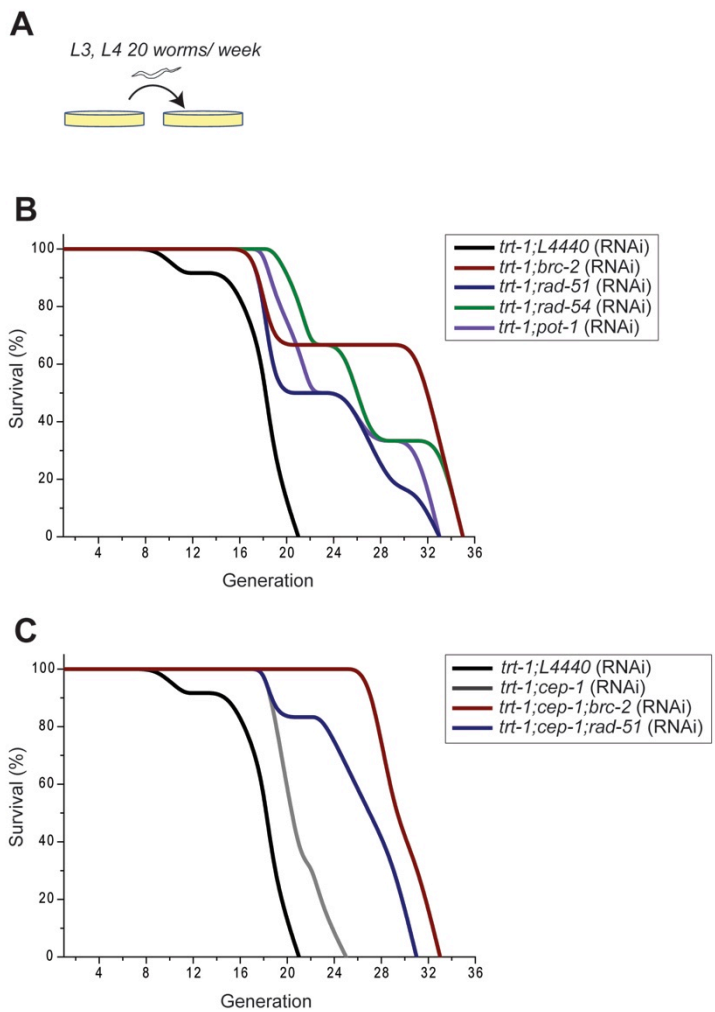

Figure 21 *brc-2* knock-downed *trt-1 (ok410)* shows extended generation propagation

Figure 21. *brc-2* knock-downed *trt-1(ok410)* shows extended generation propagation.

A. Illustration of experimental scheme; *trt-1(ok410)* fed RNAi expressing HT115 (DE) bacteria. 20 worms at L3 or L4 stage were transferred (more than 12 sets per genotypes, two or 1.5 generation per week).

B, C. Graph showing the survival rates (%) of feeding RNAi of indicated genes in *trt-1 (ok410)*.

B. *trt-1;L4440* (RNAi) (empty vector, black), *trt-1;brc-2* (RNAi) (wine), *trt-1;rad-51* (RNAi) (navy), *trt-1;rad-54* (RNAi) (emerald), *trt-1;pot-1* (RNAi) (violet),

C. *trt-1;L4440* (RNAi) (empty vector, black), *trt-1;cep-1 (RNAi)* (gray), *trt-1;cep-1 (RNAi); brc-2* (RNAi) (wine), *trt-1; cep-1 (RNAi); rad-51* (RNAi) (navy).

Graphs were plotted using B-spline (OriginPro 8.6). X-axis, generations; Y-axis, percentage of survival

III-3-2. BRCA2 RNAi in telomerase-mutant worms exhibits longer telomeres length than *trt-1* mutant worms.

To assess whether the extended propagation of *trt-1 (ok410)* fed *brc-2* RNAi is associated with the maintenance of telomere length, I performed STELA (Singel TElomere Length Analysis) assay **(FIGURE 22A)**. STELA assay is a ligation PCR-based method for measuring telomere length. STELA assay allows quantification of specific chromosome ends that enables quantification of both mean telomere length per cell and the percentage of short telomere population, beside TRF (Telomere restriction fragment; Telomeric southern blot) analysis only provides the estimated mean telomere length (Vera and Blasco, 2012). STELA assay also used for determining the identity of the strand terminal nucleotide and estimating the G-, C-overhang population by using various telorrete (Sfeir et al., 2005).

In generation 17, *trt-1 (ok410)* fed *L4440* RNAi survival rates were dropped markedly. Thus, I performed STELA assay in generation 17, to investigate that the difference in propagation would be coming from the difference in telomere length. The STELA result shows that the telomere lengths of *trt-1 (ok410)* fed *rad-51* RNAi or *brc-2* RNAi were comparable to N2 (WT), although *trt-1(ok410)* fed *L4440* RNAi showed extremely short telomere lengths **(FIGURE 22B)**. This suggests that extended propagation in *trt-1*

(ok410) fed *brc-2* RNAi would be through lengthening of telomere. Furthermore, the intensity and number of STELA products in *trt-1 (ok410)* fed *brc-2* RNAi or *rad-51* RNAi were much lower than in *trt-1 (ok410)* fed *L4440* or N2 (WT) **(FIGURE 22B)**. This may result from the difference of C/G-overhang population in *trt-1 (ok410)* fed *brc-2* RNAi or *rad-51* RNAi, since STELA assay was performed by using telorrete which bind to C-strand end in G-overhang. Related to this, it has been reported that depletion of HR factor in ALT cells induces the increase of C-overhang population (Oganesian and Karlseder, 2011). Therefore, measuring overhang population in *trt-1 (ok410)* fed *brc-2* or *rad-51* RNAi is required for analyzing ALT-phenotypes in BRCA2-deficient condition.

Figure 22.

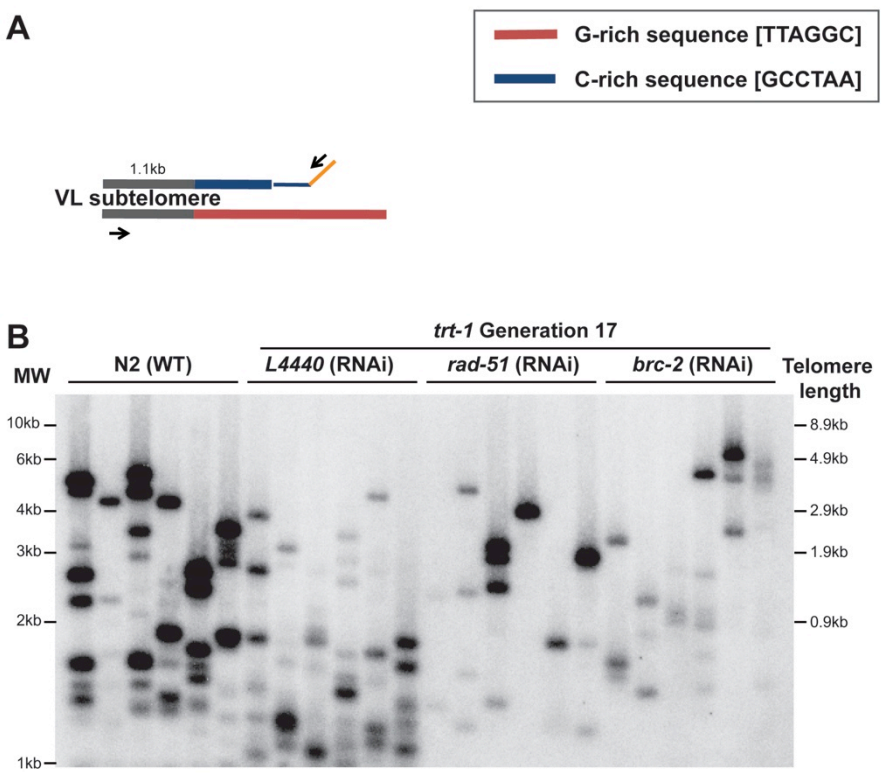

Figure 22 *brc-2* knock-downed *trt-1 (ok410)* maintains telomere lengths

Figure 22. *brc-2* knock-downed *trt-1(ok410)* maintains telomere length.

A. Schematic of the ends of *C. elegans* V chromosomes-L arms and the STELA (Single TElomere Length Analysis) assay. Telorerres (a thin navy + orange bar) and 5' end (C-rich sequence, a thick navy bar) are ligated together. PCR used for amplifying telomere and subtelomere regions.

B. Product of STELA using the indicated worms. N2 (WT) and *trt-1* Generation 17 (G17) obtained from Figure 21 A were used for analysis. Telorerres were used for 6 independent assays and the products were run in separated lanes. Note that *trt-1;rad-51* (RNAi) and *trt-1;brc-2* (RNAi) contains much longer telomeres than *trt-1;L4440* (RNAi, empty vector).

III-3-3. BRCA2 RNAi in telomerase-mutant worms induces C-circles, a hallmark of ALT.

Next, I measured C-circles, which is the most robust marker for ALT, in *trt-1 (ok410)* fed *brc-2* RNAi to address BRCA2 deficiency is related with ALT onset. Through C-, G-circle assay, we can detect ALT-specific single stranded telomeric DNA by using ϕ29 DNA polymerase, which is used for the elongation of self-primed Rolling Circle Amplification (RCA) **(FIGURE 23A)**. I performed C-, G-circle assay in generation 17 of *trt-1 (ok410)* as shown above. The levels of C-circles in *trt-1 (ok410)* fed *brc-2*, *rad-51, or rad-54* RNAi were much higher than in *trt-1 (ok410)* fed *L4440* **(FIGURE 23B, C)**, although the levels of G-circles are indistinguishable **(FIGURE 23D)**.

Interestingly there is no C-, G-circle level changes in N2 fed *brc-2*, *rad-51* or *rad-54* RNAi **(FIGURE 23 E, F)**, which indicates that telomerase may depress BRCA2-depletion-induced ALT (BR2-ALT). It has been reported that unlikely to other ALT marker, C-circles are diminished in response to telomerase expression in ALT cells, which indicates that the generation mechanisms of C-circles are suppressed by telomerase. Thus we can anticipate that the mechanism of BR2-ALT would possess common features for ALT. Further studies for the mechanism of C-circle generation in BR2-

ALT would provide not only understanding for the contribution of BRCA2 in ALT onset but also insight for the ALT mechanisms.

Figure 23.

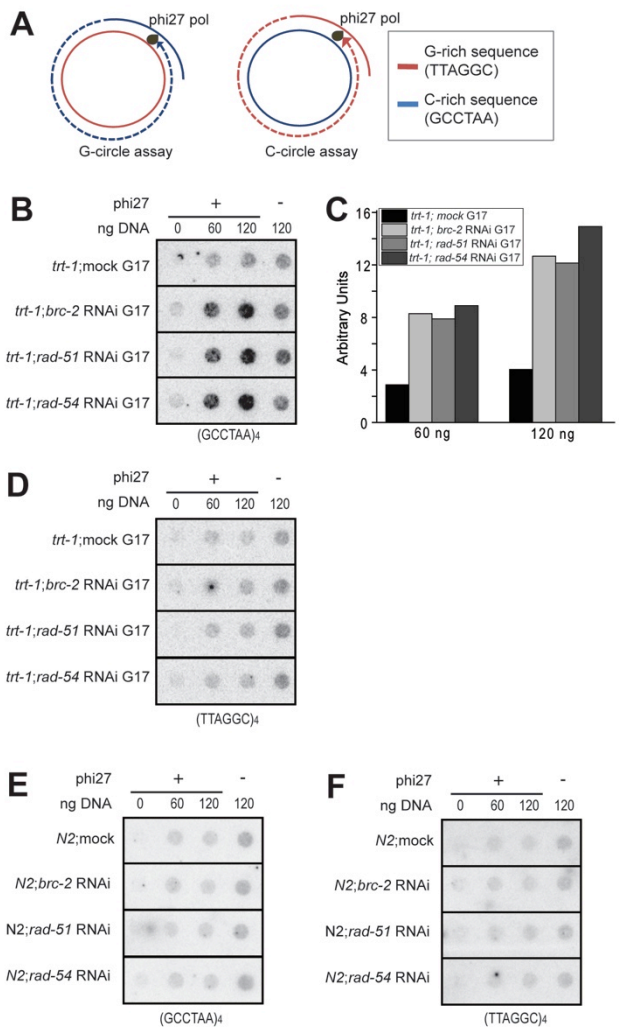

Figure 23 *brc-2* RNAi in *trt-1(ok410)* have increased C-circles, but not *brc-2* RNAi in N2 (WT)

Figure 23. *brc-2* RNAi in *trt-1(ok410)* have increased C-circles, but not *brc-2* RNAi in N2 (WT).

A. Schematic of G-, C-circle assay. Partially double stranded C-, G-circles are amplified by F29 DNA polymerase which are auto-primed by the partial complementary sequence.

B, D-F. Product of C-circle assay (B, E) and G-circle assay (D, F) using indicated worms. Dot blot of C-, G-circle assay were performed with serial dilution of genomic DNA from RNAi worms in *trt-1* G17 (B, D) or in N2 (E, F). $(GCCTAA)_4$ probe were used for C-circles detection, and $(TTAGGC)_4$ for G-circles detection.

C. Quantification of the C-circle amplified signals performed in B. X-axis, DNA concentration; Y-axis, arbitrary unit for signal intensity

V. Discussion

IV-1. The roles of BRCA2 in telomere maintenance

Dysfunctional telomeres in the absence of BRCA2

The maintenance mechanisms for telomeres have been provided by several pathways, which are mediated by shelterin proteins or DNA damage response- or repair-associated factors. I showed that BRCA2, a tumor suppressor responsible for familiar breast cancer, regulates telomere homeostasis. In the absence of BRCA2 end chromosomal fusions are increased, which is responsible for the telomere length rapid deletion. These data shows that End chromosomal fusions induced by Telomere length Rapid Deletion contribute to the genetic instability driving to tumorigenesis in BRCA2-deficient cells.

Non-Homologous End Joining (NHEJ) pathway involved in the fusion of telomeres lacking BRCA2

NHEJ pathway is composed of two pathways: classical NHEJ (C-NHEJ, Ku70/86 and DNA ligase IV (Lig 4)-Xrcc4 complex dependent) and alternative NHEJ (A-NHEJ, DNA ligase III and PARP-1 dependent). In contrast to C-NHEJ, A-NHEJ is the joining reaction, which uses short tracks

of micro-homology at the 3′ overhang junction. End joining reactions at the telomeres are separated by two ways, ATM dependent C-NHEJ (suppressed by TRF2/RAP1, mediated by C-NHEJ factors, such as 53BP1 and KU70), and ATR dependent A-NHEJ (suppressed by POT1/TPP1) (Sfeir and de Lange, 2012). Since Natural telomere attrition induced end joining is not mediated by C-NHEJ, it is speculated that A-NHEJ is used to fuse naturally shortened telomeres (Rai et al., 2010). Hence A-NHEJ relies on HR factors for searching short tracks of micro-homology at the 3′ overhang junctions, A-NHEJ would be suppressed at the telomeres in the absence of BRCA2. Although we showed that BRCA2 depletion does not change binding affinity of TRF1 and TRF2 to the telomeres **(FIGURE 19A),** ATM dependent DNA damage response marker such as 53BP1 much abundant at the telomeres, which indicates that C-NHEJ would be more responsible for telomeric end joining in the absence of BRCA2 than A-NHEJ **(FIGURE 12)**. Though more investigations are required for verifying the NHEJ pathway in the absence of BRCA2, I speculate that BRCA2-depletion induced end joining would be mediated by C-NHEJ.

BRCA2 is required for telomere replication fidelity.

We showed that BRCA2 has a role in facilitating G-rich lagging strand synthesis at telomeres, by blocking stalled replication fork degradation. I also

showed that telomeric DNA replication fidelity is impaired in BRCA2-lacking condition. Theses data suggest that BRCA2 is required for efficient and complete DNA replication process in telomere, which is responsible for the dysfunctional telomere in Brca2-depleted cells.

Since telomeres have limited numbers of replication origin, most replication forks at the telomeres are originated from subtelomere regions. Due to these reasons, Telomere replication is usually unidirectional and telomeres possesses G-rich lagging strands as parental lagging strand, which exposed as single strands between okazaki fragments can adopt G-quadruplex. Thus Telomeres are prone to face difficulty in the processing of DNA replication and cannot be rescued by a converging another replication fork. Hence it is considered that the mechanisms for the maintenance of replication fidelity are crucial for the telomeres than other genome regions. As described above, BRCA2 protects the nascent strand at stalled replication fork from MRE11-dependent resection. In the absence of BRCA2, fragile telomere expression is related to lagging strand problem **(FIGURE 16)**. The increase of G-rich single stranded DNA in the absence of BRCA2 is associated with the resection of nascent strand of the G-rich lagging strands during telomere replication **(FIGURE 18)**. Replication fork protection problem in telomeres would be more profound compared to the non-telomeric region in BRCA2-knockout MEFs. Moreover these defects

followed by incomplete termination of S phase **(FIGURE 19)**, represented by dysfunctional telomeres.

End capping problems in the BRCA2-deficient condition

The function of BRCA2 in DNA metabolism can be classified into two categories. First group is error free DSBs repair pathway, homologous recombination (BRCA2, RAD51 and RAD54 proteins are participated in this process). Second group is the protection mechanism for blocking nascent DNA resection in stalled replication fork (BRCA2, RAD51 proteins are participated in this process, but not RAD54). It has been reported that telomere length rapid deletion but not telomere replication problems in Rad54-deficient MEFs (Jaco et al., 2003). Thus it is possible that telomere rapid deletion in BRCA2-deficient cells would be responsible for HR defects as well as defects in protection of stalled DNA replication fork. In addition to Rad54 MEFs analysis, it has been reported that BRCA2-deficient cells showed Extra-chromosomal telomere repeats (ECTR) (Bodvarsdottir et al., 2012), and we also observed the increase of ECTR in Brca2-deficient MEFs (unpublished data from our group). It is thought that T-circles are represented as ECTR, which is related with the existence of T-circles in Brca2-deficient MEFs (unpublished data from our group). Since T-circle generation is associated with junction resolution of T-loop, which is responsible for end capping

problem from HR-defects **(FIGURE 5)**, T-circles generation in Brca2-deficient cells result from end capping problems induced by HR, which might be the additional trigger for Telomere length Rapid Deletion in Brca2-deficient MEFs. Further studies are required to investigate the mechanisms of BRCA2 for telomere end capping.

ALT induction in BRCA2 lacking condition

The extended propagation in *trt-1 (ok410)* fed *brc-2* RNAi result from the onset of ALT mechanisms. The mechanisms for BRCA2-deficiency induced ALT are not identified yet. But the hypothesis that I suggest for explaining the BRCA2-deficiency induced ALT will be discussed in next chapter (**IV-3. T-circle mediated rolling circle amplification hypothesis**).

IV-2. Contribution of telomere erosions and ALT in the neoplastic transformation of BRCA2-deficient cells

Germ-line mutations in *BRCA2* predispose to the cancers. Since BRCA2 is required for the maintenance of genetic integrity, absence of BRCA2 results in the accumulation of spontaneous gross chromosomal rearrangement (GCR), such as translocations, deletions, inversions and amplifications, which would be result from defects in HR and Stalled replication fork protection (Yu et al., 2000). BRCA2 also regulates the spindle assembly checkpoint through reinforcement of BubR1 acetylation, which is responsible for the chromosomal number instability in BRCA2-deficient cells (Choi et al., 2012). It has been thought that such genetic instabilities act synergistically, which would promote tumorigenesis in BRCA2 deficient cells. However these defect, itself does not sufficient for explaining the procedure of neoplastic transformation induced by BRCA2-mutation.

I suggest that the alteration of telomere homeostasis induced by BRCA2-deficiency can explain the features of BRCA2-mutated cancer, early onset and severe genetic instability (illustrated in **FIGURE 24)**. BRCA2-deficiency in early stages of tumorigenesis would promote the acceleration of telomere erosion and accumulation of dysfunctional telomeres at a faster rate than BRCA2-normal condition (**FIGURE 24 (1), ~ M1)**. BRCA2-deficiency in late stages of tumorigenesis makes cells acquire telomere maintenance

mechanism for neoplastic transformation through ALT mechanism **(FIGURE 24 (2), M2)**. It has been reported that BRCA2-mutated tumor samples have dysfunctional telomeres and shorten telomere compared to sporadic tumor samples (Bodvarsdottir et al., 2012). Moreover, it would be worth to determining if BRCA2-mutated cancer cells maintain their telomere length by ALT mechanism.

Figure 24.

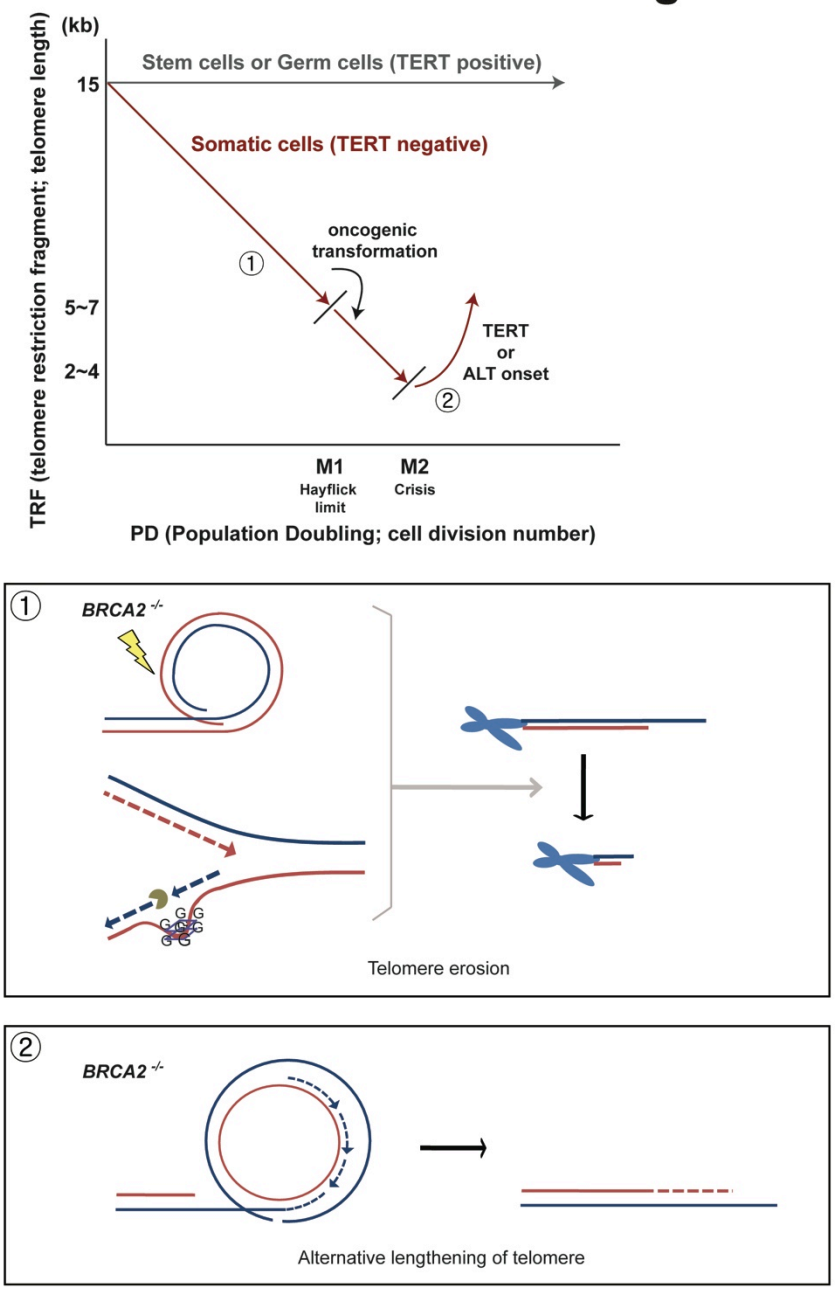

Figure 24 Model for the contributions of telomere erosions and ALT to the neoplastic transformation of BRCA2-mutated cancer

Figure 24. Model for the contributions of telomere erosions and ALT to the neoplastic transformation of BRCA2-mutated cancer

Schematic of alternation of telomere homeostasis in neoplastic transformation induced by BRCA2-mutation
(1). In early stages of tumorigenesis (~M1, 1), the rate of telomere length shortening is much faster in BRCA2-mutated cells than in BRCA2-normal cells, since BRCA2 is required for telomere maintenance. Acceleration of telomere length shortening and genetic instability induced by BRCA2 deficiency would be resulted in promoting tumorigenesis.
(2). In late stages of tumorigenesis (M2, 2), BRCA2-mutation makes cells acquire telomere maintenance mechanism for neoplastic transformation through ALT mechanism, which would increase the chances for overcoming the crisis.

IV-3. T-circle-mediated rolling circle amplification may be responsible for ALT

Here, I propose the T-circle mediated rolling circle amplification hypothesis for explaining the BRCA2-deficiency induced ALT (BR2-ALT) **(FIGURE 25)**. In the absence of BRCA2, T-circles are increased in response to telomere uncapping problem (data not shown, unpublished data). It has been reported that T-circle generation mechanisms are accompanied by C-overhang generation (Pickett et al., 2011), which would be mediated by unknown factor, endonuclease X (mediates the resolution of T-loop junction by cleaving) and exonuclease Y (mediates C-overhang generation by resection). The increases of C-overhang upon depletion of HR factors (RAD51, RAD52) in ALT cells (Oganesian and Karlseder, 2011) would be resulted from uncapping problems and unregulated resection by exonuclease Y in ALT cells. Moreover, it is possible that unknown exonuclease Y is responsible for C-overhang generation in ALT cells. It is also possible that telomerase might suppress C-overhang generation, since no overhang difference in Brca2-deficient MEFs (telomerase positive) **(FIGURE 18 A)**. Moreover, there were no C-circles in Brca2-deficient MEFs (data not shown) and N2 fed *brc-2* RNAi **(FIGURE 23)**.

Collectively, I can assume that T-circle and C-overhang generation would be prior to C-circle generation. Thus, I suggest that BR2-ALT would be done by the T-circle mediated rolling circle amplification as illustrated in (**FIGURE 25,** Note the procedure of circles generation). T-circle RCA invaded by C-overhang results in C-circle generation is main difference of my hypothesis from others (T-circle RCA invaded by G-overhang; cannot explain the C-circle generation mechanism). At this time, it is not sufficient to support this hypothesis. More investigations are required for verifying TMRCA hypothesis.

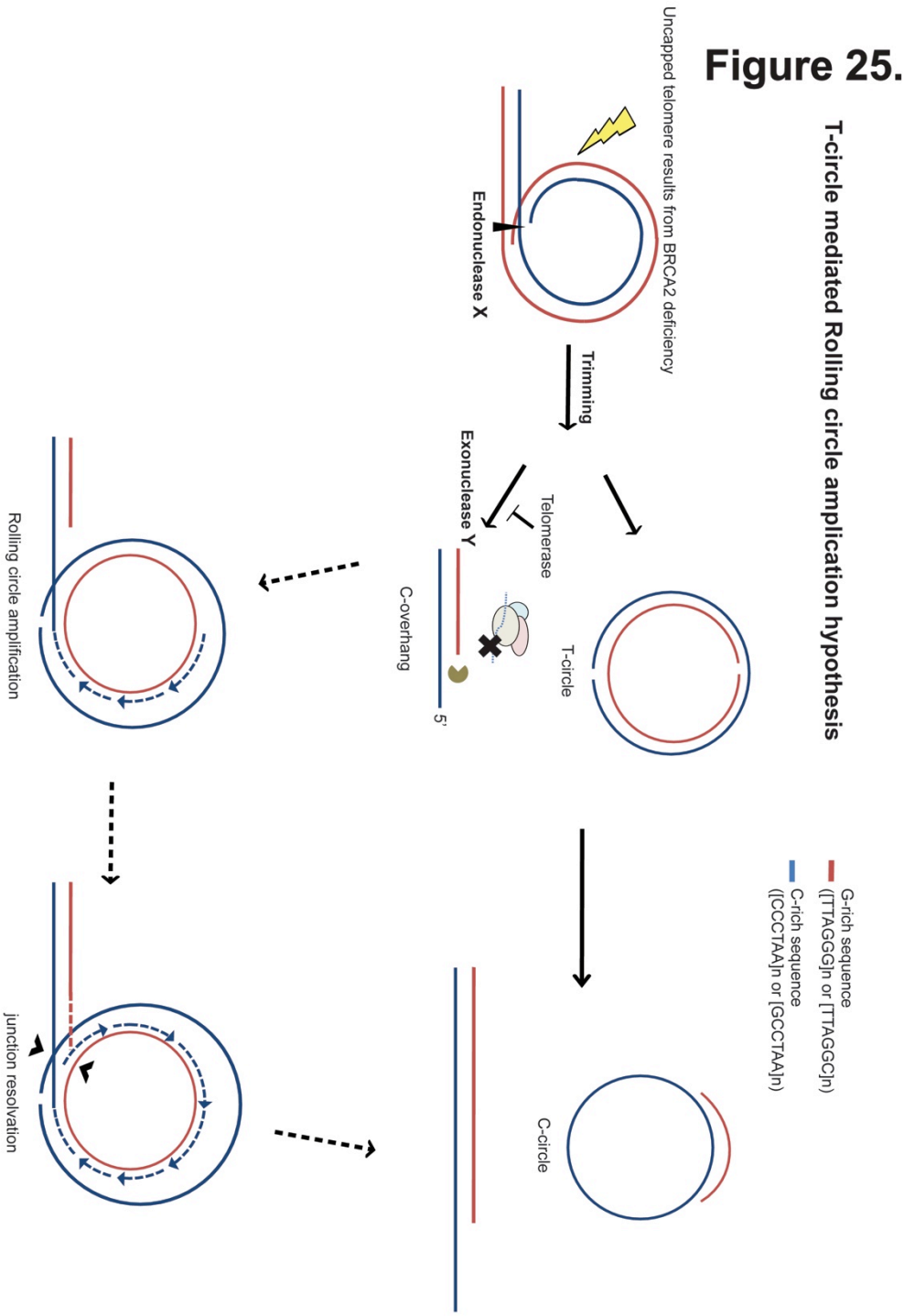

Figure 25 T-circle-mediated rolling circle amplification(TMRCA) hypothesis

Figure 25. T-circle-mediated rolling circle amplification (TMRCA) hypothesis

Schematic for T-circle mediated rolling circle amplification hypothesis. BRCA2-depletion induces uncapped telomere. Uncapped telomere result in the generation of T-loop sized T-circles and C-overhangs, which is mediated by endonuclease X and exonuclease Y. T-circles are invaded by C-overhang, then the rolling circle amplifications (RCA) are proceeded. After C-overhangs are elongated by RCA, G-rich complementary sequences are synthesized by DNA polymerases. After the length of telomere end has been extended, the junction would be resolved, which result in C-circle generation, a robust maker for ALT.

V. References

Arnoult, N., Saintome, C., Ourliac-Garnier, I., Riou, J.F., and Londono-Vallejo, A. (2009). Human POT1 is required for efficient telomere C-rich strand replication in the absence of WRN. Genes Dev *23*, 2915-2924.

Artandi, S.E., and DePinho, R.A. (2010). Telomeres and telomerase in cancer. Carcinogenesis *31*, 9-18.

Bodvarsdottir, S.K., Steinarsdottir, M., Bjarnason, H., and Eyfjord, J.E. (2012). Dysfunctional telomeres in human BRCA2 mutated breast tumors and cell lines. Mutation research *729*, 90-99.

Brault, M.E., and Autexier, C. (2011). Telomeric recombination induced by dysfunctional telomeres. Molecular biology of the cell *22*, 179-188.

Cesare, A.J., and Reddel, R.R. (2010). Alternative lengthening of telomeres: models, mechanisms and implications. Nature reviews Genetics *11*, 319-330.

Chin, K., de Solorzano, C.O., Knowles, D., Jones, A., Chou, W., Rodriguez, E.G., Kuo, W.L., Ljung, B.M., Chew, K., Myambo, K.*, et al.* (2004). In situ analyses of genome instability in breast cancer. Nat Genet *36*, 984-988.

Choi, E., Choe, H., Min, J., Choi, J.Y., Kim, J., and Lee, H. (2009). BubR1 acetylation at prometaphase is required for modulating APC/C activity and timing of mitosis. Embo J *28*, 2077-2089.

Choi, E., Park, P.G., Lee, H.O., Lee, Y.K., Kang, G.H., Lee, J.W., Han, W., Lee, H.C., Noh, D.Y., Lekomtsev, S.*, et al.* (2012). BRCA2 fine-tunes the spindle assembly checkpoint through reinforcement of BubR1 acetylation. Developmental cell *22*, 295-308.

Cimino-Reale, G., Pascale, E., Alvino, E., Starace, G., and D'Ambrosio, E. (2003). Long telomeric C-rich 5'-tails in human replicating cells. J Biol Chem *278*, 2136-2140.

Cimino-Reale, G., Pascale, E., Battiloro, E., Starace, G., Verna, R., and D'Ambrosio, E. (2001). The length of telomeric G-rich strand 3'-overhang measured by oligonucleotide ligation assay. Nucleic acids research *29*, E35.

Crabbe, L., Jauch, A., Naeger, C.M., Holtgreve-Grez, H., and Karlseder, J. (2007). Telomere dysfunction as a cause of genomic instability in Werner syndrome. Proc Natl Acad Sci U S A *104*, 2205-2210.

Daboussi, F., Courbet, S., Benhamou, S., Kannouche, P., Zdzienicka, M.Z., Debatisse, M., and Lopez, B.S. (2008). A homologous recombination defect affects replication-fork progression in mammalian cells. J Cell Sci *121*, 162-166.

Darzynkiewicz, Z., and Juan, G. (2001). Analysis of DNA content and BrdU incorporation. Curr Protoc Cytom *Chapter 7*, Unit 7 7.

de Lange, T. (2004). T-loops and the origin of telomeres. Nature reviews Molecular cell biology *5*, 323-329.
Dimitrova, D.S., and Gilbert, D.M. (2000). Temporally coordinated assembly and disassembly of replication factories in the absence of DNA synthesis. Nat Cell Biol *2*, 686-694.
Esashi, F., Christ, N., Gannon, J., Liu, Y., Hunt, T., Jasin, M., and West, S.C. (2005). CDK-dependent phosphorylation of BRCA2 as a regulatory mechanism for recombinational repair. Nature *434*, 598-604.
Esashi, F., Galkin, V.E., Yu, X., Egelman, E.H., and West, S.C. (2007). Stabilization of RAD51 nucleoprotein filaments by the C-terminal region of BRCA2. Nat Struct Mol Biol *14*, 468-474.
Evers, B., and Jonkers, J. (2006). Mouse models of BRCA1 and BRCA2 deficiency: past lessons, current understanding and future prospects. Oncogene *25*, 5885-5897.
Fackenthal, J.D., and Olopade, O.I. (2007). Breast cancer risk associated with BRCA1 and BRCA2 in diverse populations. Nat Rev Cancer *7*, 937-948.
Friedman, L.S., Thistlethwaite, F.C., Patel, K.J., Yu, V.P., Lee, H., Venkitaraman, A.R., Abel, K.J., Carlton, M.B., Hunter, S.M., Colledge, W.H.*, et al.* (1998). Thymic lymphomas in mice with a truncating mutation in Brca2. Cancer research *58*, 1338-1343.
Galkin, V.E., Esashi, F., Yu, X., Yang, S., West, S.C., and Egelman, E.H. (2005). BRCA2 BRC motifs bind RAD51-DNA filaments. Proc Natl Acad Sci U S A *102*, 8537-8542.
Gilson, E., and Geli, V. (2007). How telomeres are replicated. Nat Rev Mol Cell Biol *8*, 825-838.
Griffith, J.D., Comeau, L., Rosenfield, S., Stansel, R.M., Bianchi, A., Moss, H., and de Lange, T. (1999). Mammalian telomeres end in a large duplex loop. Cell *97*, 503-514.
Hackett, J.A., and Greider, C.W. (2002). Balancing instability: dual roles for telomerase and telomere dysfunction in tumorigenesis. Oncogene *21*, 619-626.
Hashimoto, Y., Chaudhuri, A.R., Lopes, M., and Costanzo, V. (2010). Rad51 protects nascent DNA from Mre11-dependent degradation and promotes continuous DNA synthesis. Nat Struct Mol Biol *17*, 1305-1311.
Henson, J.D., Cao, Y., Huschtscha, L.I., Chang, A.C., Au, A.Y., Pickett, H.A., and Reddel, R.R. (2009). DNA C-circles are specific and quantifiable markers of alternative-lengthening-of-telomeres activity. Nature biotechnology *27*, 1181-1185.
Im, S.H., and Lee, J. (2005). PLP-1 binds nematode double-stranded telomeric DNA. Molecules and cells *20*, 297-302.
Jaco, I., Munoz, P., Goytisolo, F., Wesoly, J., Bailey, S., Taccioli, G., and Blasco, M.A. (2003). Role of mammalian Rad54 in telomere length maintenance. Molecular and cellular biology *23*, 5572-5580.

Joeng, K.S., Song, E.J., Lee, K.J., and Lee, J. (2004). Long lifespan in worms with long telomeric DNA. Nature genetics *36*, 607-611.
Jonkers, J., Meuwissen, R., van der Gulden, H., Peterse, H., van der Valk, M., and Berns, A. (2001). Synergistic tumor suppressor activity of BRCA2 and p53 in a conditional mouse model for breast cancer. Nat Genet *29*, 418-425.
Kennedy, R.D., and D'Andrea, A.D. (2005). The Fanconi Anemia/BRCA pathway: new faces in the crowd. Genes Dev *19*, 2925-2940.
Lackner, D.H., Raices, M., Maruyama, H., Haggblom, C., and Karlseder, J. (2012). Organismal propagation in the absence of a functional telomerase pathway in Caenorhabditis elegans. The EMBO journal *31*, 2024-2033.
Liu, J., Doty, T., Gibson, B., and Heyer, W.D. (2010). Human BRCA2 protein promotes RAD51 filament formation on RPA-covered single-stranded DNA. Nature structural & molecular biology *17*, 1260-1262.
McNees, C.J., Tejera, A.M., Martinez, P., Murga, M., Mulero, F., Fernandez-Capetillo, O., and Blasco, M.A. (2010). ATR suppresses telomere fragility and recombination but is dispensable for elongation of short telomeres by telomerase. J Cell Biol *188*, 639-652.
Meier, B., Clejan, I., Liu, Y., Lowden, M., Gartner, A., Hodgkin, J., and Ahmed, S. (2006). trt-1 is the Caenorhabditis elegans catalytic subunit of telomerase. PLoS genetics *2*, e18.
Min, J., Park, P.G., Ko, E., Choi, E., and Lee, H. (2007). Identification of Rad51 regulation by BRCA2 using Caenorhabditis elegans BRCA2 and bimolecular fluorescence complementation analysis. Biochemical and biophysical research communications *362*, 958-964.
Morrish, T.A., and Greider, C.W. (2009). Short telomeres initiate telomere recombination in primary and tumor cells. PLoS Genet *5*, e1000357.
Oganesian, L., and Karlseder, J. (2011). Mammalian 5' C-rich telomeric overhangs are a mark of recombination-dependent telomere maintenance. Molecular cell *42*, 224-236.
Park, M.C., Park, D., Lee, E.K., Park, T., and Lee, J. (2010). Genomic analysis of the telomeric length effect on organismic lifespan in Caenorhabditis elegans. Biochemical and biophysical research communications *396*, 382-387.
Patel, K.J., Yu, V.P., Lee, H., Corcoran, A., Thistlethwaite, F.C., Evans, M.J., Colledge, W.H., Friedman, L.S., Ponder, B.A., and Venkitaraman, A.R. (1998). Involvement of Brca2 in DNA repair. Molecular cell *1*, 347-357.
Pellegrini, L., and Venkitaraman, A. (2004). Emerging functions of BRCA2 in DNA recombination. Trends Biochem Sci *29*, 310-316.
Pellegrini, L., Yu, D.S., Lo, T., Anand, S., Lee, M., Blundell, T.L., and Venkitaraman, A.R. (2002). Insights into DNA recombination from the structure of a RAD51-BRCA2 complex. Nature *420*, 287-293.

Pennarun, G., Hoffschir, F., Revaud, D., Granotier, C., Gauthier, L.R., Mailliet, P., Biard, D.S., and Boussin, F.D. (2010). ATR contributes to telomere maintenance in human cells. Nucleic Acids Res *38*, 2955-2963.
Petermann, E., Orta, M.L., Issaeva, N., Schultz, N., and Helleday, T. (2010). Hydroxyurea-stalled replication forks become progressively inactivated and require two different RAD51-mediated pathways for restart and repair. Mol Cell *37*, 492-502.
Pickett, H.A., Henson, J.D., Au, A.Y., Neumann, A.A., and Reddel, R.R. (2011). Normal mammalian cells negatively regulate telomere length by telomere trimming. Human molecular genetics *20*, 4684-4692.
Pickett, H.A., and Reddel, R.R. (2012). The role of telomere trimming in normal telomere length dynamics. Cell Cycle *11*, 1309-1315.
Poon, S.S., and Lansdorp, P.M. (2001). Quantitative fluorescence in situ hybridization (Q-FISH). Curr Protoc Cell Biol *Chapter 18*, Unit 18 14.
Rai, R., Zheng, H., He, H., Luo, Y., Multani, A., Carpenter, P.B., and Chang, S. (2010). The function of classical and alternative non-homologous end-joining pathways in the fusion of dysfunctional telomeres. The EMBO journal *29*, 2598-2610.
Rizzo, A., Salvati, E., Porru, M., D'Angelo, C., Stevens, M.F., D'Incalci, M., Leonetti, C., Gilson, E., Zupi, G., and Biroccio, A. (2009). Stabilization of quadruplex DNA perturbs telomere replication leading to the activation of an ATR-dependent ATM signaling pathway. Nucleic Acids Res *37*, 5353-5364.
Rosche, W.A., Trinh, T.Q., and Sinden, R.R. (1995). Differential DNA secondary structure-mediated deletion mutation in the leading and lagging strands. Journal of bacteriology *177*, 4385-4391.
Royle, N.J., Mendez-Bermudez, A., Gravani, A., Novo, C., Foxon, J., Williams, J., Cotton, V., and Hidalgo, A. (2009). The role of recombination in telomere length maintenance. Biochemical Society transactions *37*, 589-595.
Schlacher, K., Christ, N., Siaud, N., Egashira, A., Wu, H., and Jasin, M. (2011). Double-strand break repair-independent role for BRCA2 in blocking stalled replication fork degradation by MRE11. Cell *145*, 529-542.
Sfeir, A., and de Lange, T. (2012). Removal of shelterin reveals the telomere end-protection problem. Science *336*, 593-597.
Sfeir, A., Kosiyatrakul, S.T., Hockemeyer, D., MacRae, S.L., Karlseder, J., Schildkraut, C.L., and de Lange, T. (2009). Mammalian telomeres resemble fragile sites and require TRF1 for efficient replication. Cell *138*, 90-103.
Sfeir, A.J., Chai, W., Shay, J.W., and Wright, W.E. (2005). Telomere-end processing the terminal nucleotides of human chromosomes. Molecular cell *18*, 131-138.
Shivji, M.K., Davies, O.R., Savill, J.M., Bates, D.L., Pellegrini, L., and Venkitaraman, A.R. (2006). A region of human BRCA2 containing multiple

BRC repeats promotes RAD51-mediated strand exchange. Nucleic Acids Res *34*, 4000-4011.
Stewart, S.A., Ben-Porath, I., Carey, V.J., O'Connor, B.F., Hahn, W.C., and Weinberg, R.A. (2003). Erosion of the telomeric single-strand overhang at replicative senescence. Nat Genet *33*, 492-496.
Takai, H., Smogorzewska, A., and de Lange, T. (2003). DNA damage foci at dysfunctional telomeres. Current biology : CB *13*, 1549-1556.
Tavtigian, S.V., Simard, J., Rommens, J., Couch, F., Shattuck-Eidens, D., Neuhausen, S., Merajver, S., Thorlacius, S., Offit, K., Stoppa-Lyonnet, D*., et al.* (1996). The complete BRCA2 gene and mutations in chromosome 13q-linked kindreds. Nat Genet *12*, 333-337.
Trinh, T.Q., and Sinden, R.R. (1991). Preferential DNA secondary structure mutagenesis in the lagging strand of replication in E. coli. Nature *352*, 544-547.
Venkitaraman, A.R. (2002). Cancer susceptibility and the functions of BRCA1 and BRCA2. Cell *108*, 171-182.
Venkitaraman, A.R. (2004). Tracing the network connecting BRCA and Fanconi anaemia proteins. Nat Rev Cancer *4*, 266-276.
Venkitaraman, A.R. (2009). Linking the cellular functions of BRCA genes to cancer pathogenesis and treatment. Annu Rev Pathol *4*, 461-487.
Vera, E., and Blasco, M.A. (2012). Beyond average: potential for measurement of short telomeres. Aging *4*, 379-392.
Verdun, R.E., and Karlseder, J. (2006). The DNA damage machinery and homologous recombination pathway act consecutively to protect human telomeres. Cell *127*, 709-720.
Wang, B., Matsuoka, S., Carpenter, P.B., and Elledge, S.J. (2002). 53BP1, a mediator of the DNA damage checkpoint. Science *298*, 1435-1438.
Wang, R.C., Smogorzewska, A., and de Lange, T. (2004). Homologous recombination generates T-loop-sized deletions at human telomeres. Cell *119*, 355-368.
Wang, Y., Erdmann, N., Giannone, R.J., Wu, J., Gomez, M., and Liu, Y. (2005). An increase in telomere sister chromatid exchange in murine embryonic stem cells possessing critically shortened telomeres. Proc Natl Acad Sci U S A *102*, 10256-10260.
West, S.C. (2003). Molecular views of recombination proteins and their control. Nat Rev Mol Cell Biol *4*, 435-445.
Wooster, R., Bignell, G., Lancaster, J., Swift, S., Seal, S., Mangion, J., Collins, N., Gregory, S., Gumbs, C., and Micklem, G. (1995). Identification of the breast cancer susceptibility gene BRCA2. Nature *378*, 789-792.
Wright, W.E., Piatyszek, M.A., Rainey, W.E., Byrd, W., and Shay, J.W. (1996). Telomerase activity in human germline and embryonic tissues and cells. Developmental genetics *18*, 173-179.

Wu, L., Multani, A.S., He, H., Cosme-Blanco, W., Deng, Y., Deng, J.M., Bachilo, O., Pathak, S., Tahara, H., Bailey, S.M.*, et al.* (2006). Pot1 deficiency initiates DNA damage checkpoint activation and aberrant homologous recombination at telomeres. Cell *126*, 49-62.
Yang, Q., Zheng, Y.L., and Harris, C.C. (2005). POT1 and TRF2 cooperate to maintain telomeric integrity. Mol Cell Biol *25*, 1070-1080.
Yu, V.P., Koehler, M., Steinlein, C., Schmid, M., Hanakahi, L.A., van Gool, A.J., West, S.C., and Venkitaraman, A.R. (2000). Gross chromosomal rearrangements and genetic exchange between nonhomologous chromosomes following BRCA2 inactivation. Genes Dev *14*, 1400-1406.

VI. 국문초록

유방암은 여성에게서 가장 많이 발생하는 암으로 전세계적으로 천만명 이상이 이로 인해 고통을 받고 있다. 대부분은 산발적 발생 양상을 띄나 10% 정도는 유전적으로 연관성이 있을 것으로 추정되고 있다. BRCA 유전자는 가족력이 있는 유방암 환자군에서 생식선 돌연변이로 인해 암 발생이 유발되는 유전자로 클로닝 되었다. BRCA 유전자인 BRCA2 는 암 억제인자로서 BRCA2 의 돌연변이를 갖고 있는 환자군은 높은 확률로 유방암, 난소암, 췌장암에 걸린다고 알려져 있다. BRCA2 의 분자적 기능은 DNA metabolism 관점에서 recombinase Rec A orthologue 인 Rad51 의 조절을 통해 homologous recombination 을 조절하고 Stalled DNA replication fork 를 MRE11 에 의한 resection 으로 부터 보호한다. 이처럼 BRCA2 는 유전체 안정성 유지에 필수적임을 알 수 있다. BRCA2 가 없는 세포의 가장 큰 특징은 염색체 불안정성 - 염색체의 구조와 수의 이상 - 을 보인다는 것이다. 뿐만 아니라 본 연구와 관련하여 연구실에서는 BRCA2 가 없는 세포에서 염색체 말단간의 결합을 관찰 한 바 있다. 이러한 염색체 말단간의 결합은 텔로미어의 이상에서 유래 되었을 가능성을 생각해 볼 수 있다.

본 연구 결과, BRCA2 의 결손은 염색체 말단간의 결합의 증가를 가져왔으며, Telomere-FISH 를 하였을 때 텔로미어 시그널이 보이지 않는 Signal free end 가 증가하였음을 관찰하였다. 또한 결합된 염색체가 anaphase 시기에 서로 다른 극으로 끌려감으로서 나타나는 현상인 Anaphase bridge 가 관찰 되었다. 이러한 현상은 Q-FISH 를 통해 BRCA2 의 결손이 텔로미어 길이의 급격한 감소를 가져온다는 결과를 통해 BRCA2 의 결손에 의해 급격하게 짧아진 텔로미어가 염색체 말단간의 결합을 유도 되었음을 보여준다. 즉 BRCA2 의 결손으로 인한 텔로미어의 이상은 BRCA2 결손으로 유도되는 암 발생과정에서 유전체 불안정성을 가중화시켜 이는 곧 암 발생과정을 촉진할 것으로 생각할 수 있다.

BRCA2 는 텔로미어에 ATR 의존적으로 DNA 복제기에 주로 위치한다는 것을 Telomere-ChIP 을 통해서 관찰 할 수 있었다. 또한 BRCA2 의 결손은 Replication 과정중에 생기는 문제로 생각되는 Fragile telomere 의 증가를 야기 하였다. BRCA2 의 결손은 텔로미어에서의 복제과정중에 문제를 야기하는 것을 알 수 있었다. 뿐만 아니라 Fragile telomere 는 lagging strand 에서 발생하는 것을 알 수 있었으며, BRCA2 결손으로 유도되는 fragile telomere 의 발생도 lagging strand 에서 발생하는 문제와 관련이 있음을 알 수 있었다. 또한 특이하게도 BRCA2 의 결손은

복제기에 G-rich single stranded DNA 의 증가를 가져오는 것을 알 수 있었다. 이러한 사실은 BRCA2 결손은 Lagging strand 에서 single strand 로 노출되는 DNA 가 MRE11 에 의한 resection 이 발생하였다는 모델로 설명 할 수 있다.

뿐만 아니라 C. elegans 모델 시스템을 이용하여 telomerase mutant 인 trt-1 에서 BRCA2 의 orthologue 인 brc-2 를 RNAi 하였을 때, 계대가 길어지는 것을 확인 하였다. 이러한 계대의 증가는 텔로미어 길이가 유지되어 나타나는 것임을 확인하였고, telomerase 비의존적인 Alternative lengthening of telomeres (ALT)에 의해 일어났음을 C-circle assay 를 통해서 확인 할 수 있었다. 이러한 사실은 BRCA2 의 결손이 암 발생과정에서 ALT 현상을 통해 텔로미어 유지기작을 획득하는데 도움을 주었을 가능성을 제시한다고 할 수 있다.

종합을 하자면, 본 연구는 BRCA2 의 결손이 텔로미어에 미치는 영향과 암 발생과정과의 연관성에 답을 제시할 것이다. 암 발생과정 초기에 BRCA2 의 결손은 텔로미어의 이상, 텔로미어 길이의 급격한 감소를 통해 유전체 불안정성을 가중화 시킬 것이다. 그러나 crisis 와 같이 텔로미어 길이가 급격하게 짧아진 상황에서 BRCA2 의 결손은 ALT 를 유발하여 텔로미어 길이를 유지할 가능성을 더 높일 것으로 생각된다.

암 발생과정 시기, 상황에 따라 다르게 나타나는 BRCA2 에 의한 텔로미어 유지기작은 BRCA2 결손에 의한 암 발생과정에 대한 이해 뿐만 아니라 전반적인 암 발생과정에 대한 새로운 이해를 제시할 것이다.

중심어: BRCA2, 텔로미어,유전체 불안정성, 암 발생과정, ALT

학번 : 2009-30082